2010

# Interplay Between Keratin and Vimentin Expression in Oral Cancer

Mary Catherine McGinn
*Virginia Commonwealth University*

School of Medicine
Virginia Commonwealth University

This is to certify that the thesis prepared by Mary Catherine McGinn entitled INTERPLAY BETWEEN KERATIN AND VIMENTIN EXPRESSION IN ORAL CANCER has been approved by his or her committee as satisfactory completion of the thesis or dissertation requirement for the degree of Master of Science

---

Dr. Andrew Yeudall, BDS, Ph.D., Director of Thesis, Philips Institute VCU School of Dentistry

---

Dr. Zendra Zehner, Ph.D., VCU School of Medicine Department of Biochemistry

---

Dr. Joseph Feher, Ph.D., VCU School of Medicine Department of Physiology & Biophysics

---

Dr. Roland Pittman, Ph.D., VCU School of Medicine Department of Physiology & Biophysics

---

Dr. Louis DeFelice, Ph.D., Program Director, VCU School of Medicine

May 5, 2010

# INTERPLAY BETWEEN KERATIN AND VIMENTIN EXPRESSION IN ORAL CANCER

A thesis submitted in partial fulfillment of the requirements for the degree of Master of Science at Virginia Commonwealth University.

by

MARY CATHERINE MCGINN
Bachelor of Science, The College of William and Mary, 2007

Director: DR. ANDREW YEUDALL
PHILIPS INSTITUTE, VCU SCHOOL OF DENTISTRY

Virginia Commonwealth University
Richmond, Virginia
May, 2010

Acknowledgement

I would first like to acknowledge my advisor, Dr. Andrew Yeudall, for his guidance, support, and encouragement. Thank you for providing me with an amazing learning opportunity by allowing me to work in your lab. I would like to thank Dr. Zendra Zehner for her support during the coursework and collaboration on my research project. I would like to extend my appreciation to my committee members, Dr. Joseph Feher and Dr. Roland Pittman. To Dr. Hiro Miyazaki, thanks for answering questions in the lab and always providing questions to keep me thinking. Many thanks to Huixin Wang for her friendship, outstanding patience, and willingness to help all of us in the lab. I would also like to thank the other members of my lab for keeping each day exciting - Shahrzad Firouzabadian, Eunmee Lee, Mi-Yon Choi, Crystal Cunningham, Banks Allen, and Steven Christofakis. Furthermore, thanks to Emily Jumet and Brian Mahoney for being my graduate school study buddies.

Additionally, thank you to Jenny Hoyt for being my graduate school "mentor" and best friend. To Chris Smith, thank you for your friendship, support, and motivation throughout this whole experience. Thank you Aunt Carolyn for the meals, cards, and being my family here in Richmond. To my brother James, I am so proud of you and glad that we are sharing this graduation year. To my sister Malone, thanks for being the best sister and friend I could ever ask for, sharing my love of music, and always being there for me. Lastly, thank you to my parents for your endless love and support. You two

always have the best advice, and I could not have done this without you. I am blessed to have you as my role models. I love you.

# Table of Contents

Page

# List of Tables

Page

# List of Figures

Page

# List of Abbreviations

| | |
|---|---|
| 2-mercaptoethanol | 2-hydroxyethylmercaptan; ß-mercaptoethanol |
| 5-Aza-C | 5-aza-2'-deoxycytidine |
| BSA | Bovine Serum Albumin |
| cDNA | Complementary Deoxyribonucleic Acid |
| CK1a | Casein Kinase 1a |
| DAPI | 4', 6-diamidino-2-phenylindole |
| DKK | Dickkopf |
| DMEM | Dulbecco's Modification of Eagle's Medium |
| DMSO | Dimethyl Sulfoxide |
| DNA | Deoxyribonucleic Acid |
| dNTP | Deoxyribonucleotide Triphosphate |
| Dvl | Dishevelled |
| EDTA | Ethylene Diamine Tetra Acetic Acid |
| EMT | Epithelial to Mesenchymal Transition |
| FBS | Fetal Bovine Serum |
| FITC | Fluorescein Isothiocyanate |
| Fzd | Frizzled |
| GFP | Green Fluorescent Protein |
| GSK3ß | Glycogen Synthase Kinase 3ß |
| HNSCC | Head and Neck Squamous Cell Carcinoma |
| I?B | Inhibitor ?B |
| LEF | Lymphoid Enhancer Factor |
| LRP | Low-density Lipoprotein Receptor |
| MMP | Matrix Metalloprotease |
| mRNA | Messenger RNA |

| | |
|---|---|
| MTT | (3-(4,5-Dimethylthiazol-2-yl)-2,5-diphenyltetrazolium bromide |
| NaCl | Sodium Chloride |
| NaOH | Sodium Hydroxide |
| NF-?B | Nuclear Factor-?B |
| NTC | Non-targeting Control |
| PAGE | Polyacrylamide Gel Electrophoresis |
| PBS | Phosphate Buffered Saline |
| PBST | Phosphate Buffered Saline + Triton-X |
| PCR | Polymerase Chain Reaction |
| PKA | Protein Kinase A |
| PKC | Protein Kinase C |
| PMSF | Phenylmethylsulfonyl Fluoride |
| PVDF | Polyvinylidene Fluoride |
| qRT-PCR | Quantitative Real-time PCR |
| RNA | Ribonucleic Acid |
| SDS | Sodium Dodecyl Sulphate |
| sFRP | Secreted Frizzled Related Protein |
| shRNA | Short Hairpin RNA |
| TCF | T-cell factor |
| Tris | Tris (Hydroxymethyl) Methylamine |
| TTBS | Tween-Tris-Buffered Saline |
| Tween 20 | Polyoxyethylene(20)sorbitan Monolaurate |
| WIF | Wnt Inhibitory Factor |

# List of Materials

## Bacterial Media

2 x YT Medium: 1.6% tryptone, 1% yeast, and 0.5% sodium chloride, 50$\mu$g/mL kanamycin.

## Solutions for the Preparation of DNA

1. Cell Resuspension Solution: 50 mM Tris-HCl pH 7.5, 10 mM EDTA, 100 $\mu$g/mL RNaseA

2. Cell Lysis Solution: 0.2 M NaOH, 1% SDS

3. Neutralization Solution: 4.09 M guanidine hydrochloride, 0.759 M potassium acetate, 2.12 M glacial acetic acid

## Solutions for Western Blotting

1. Vimentin Lysis Buffer: 62.5 mM Tris-HCl pH6.8, 2% SDS, 5% ß-mercaptoethanol, 10% glycerol, 1 $\mu$L aprotonin, 1 $\mu$L leupeptin, 1 $\mu$L PMSF

2. 1 x SDS-PAGE: 20 mM Tris-HCl pH 7.9, 100 mM NaCl, 70 mM EDTA, 2% SDS

3. 1 x Transfer Buffer: 20 mM pH 7.9, 100 mM NaCl, 70 mM EDTA, and 20% methanol

# Abstract

INTERPLAY BETWEEN KERATIN AND VIMENTIN EXPRESSION IN ORAL CANCER

By Mary Catherine McGinn, M.S.

A thesis submitted in partial fulfillment of the requirements for the degree of Master of Science at Virginia Commonwealth University.

Virginia Commonwealth University, 2010

Major Director: Dr. Andrew Yeudall
Philips Institute, VCU School of Dentistry

Previous research in our laboratory found that inhibiting expression of vimentin, a marker of epithelial-to mesenchymal transition, inhibited cell growth and motility *in vitro* and *in vivo*. Tumors derived from vimentin knockdown cells showed features of epithelial redifferentiation and increased expression of differentiation-specific keratins. It is unknown what causes re-expression of keratins when vimentin is inhibited. Although, canonical Wnt signaling may activate NF-?B and repress of keratin and/or induce vimentin expression through ß-catenin. We hypothesize that ownregulation of differentiation-specific keratins contributes to tumor progression, mediated directly or indirectly by

expression of vimentin. Vimentin-negative HN4 cells were transfected with plasmids encoding wild-type, PKCe-phosphomimetic, or unphosphorylatable versions of vimentin. Expression of vimentin was confirmed by western blot and immunofluorescence. Effects on cell growth and motility were determined using MTT, cell proliferation, and wound-closure assays. These results indicate that mutation of vimentin PKCe-phosphorylation sites cause changes in proliferation and filament assembly. Treatment of cells with an NF-?B inhibitor or 5-Aza-C, which allows re-expression of the Wnt inhibitor DKK3, led to a decrease in proliferation. These results suggest that inhibiting Wnt signaling removes the inhibition on GSK-3ß and prevents activation of NF-?B, which decreases proliferation.

# Introduction

## Cancer and Tumor Growth

Cancer cells develop due to changes in normal controls that regulate cell proliferation and homeostasis. There are genetic regulatory systems that maintain a balance between cell birth and death through growth signals, growth inhibitory signals, and death signals (Lodish, 2004). Normal control of cell division is maintained by extracellular growth factors, and errors in generating, regulating, or recognizing these growth factors can result in cancer (Lehninger, Nelson, & Cox, 2005). Six hallmarks have been generated that classify changes leading to cancer cell growth. These six characteristics are "self sufficiency in growth signals, insensitivity to growth-inhibitory (antigrowth) signals, evasion of programmed cell death (apoptosis), limitless replicative potential, sustained angiogenesis, and tissue invasion and metastasis" (Hanahan & Weinberg, 2000). Most human tumors possess these six traits. Normal cells require growth signals before transitioning from the quiescent to proliferative state, but tumor cells are not, in many cases, dependent on these growth signals, as they frequently create their own. Many of the cell surface receptors that induce growth signals are deregulated during tumorigenesis. Additionally, normal tissues have antiproliferative signals to maintain homeostasis, and these operate through two mechanisms. One mechanism forces cells to exit the cell cycle and into a quiescent state. These cells may reenter the cell cycle in the presence of

appropriate extracellular signals. The other mechanism prevents the cell from ever proliferating again, and it enters a postmitotic state. Tumor cells have acquired mechanisms to bypass this terminal differentiation (Hanahan & Weinberg, 2000).

Mutations in two classes of genes are frequently involved in cancer. These genes are proto-oncogenes and tumor suppressor genes. Proto-oncogenes are normally involved in cell growth, but mutations can change them into oncogenes causing excessive growth (Lodish, 2004). These oncogenes can be activated by genetic or epigenetic factors. Genetic changes occur due to mutation, deletion, amplification, or translocation. A single mutational event can cause the proto-oncogene to contribute to cancer. Epigenetic factors are a result of heritable changes in the gene that operate outside changes in the DNA itself. This could be due to methylation or histone modification and may also influence the expression of oncogenes or tumor suppressor genes (Palmieri et al., 2009). On the other hand, tumor suppressor genes normally prevent growth. When mutations occur, these genes are inactivated which enables cells to proliferate with unregulated and self-sufficient growth. In order for tumor suppressor genes to contribute to cancer, both alleles must be mutated, so this requires two mutational events (Lodish, 2004). The presence of environmental carcinogens can cause changes in these tumor suppressor genes and proto-oncogenes, which results in malignant transformation of the cells. Telomerase, which is involved in immortalization, shows reactivation in approximately 90% of head and neck squamous cell carcinomas. These initial changes cause further genetic instability and lead to characteristics of malignant cells (Stadler, Patel, Couch, & Hayes, 2008).

Cancer is the result of phenotypic and genetic changes that ultimately result in aggressive behavior. A normal cell gets mutated which causes increased proliferation. Further mutations lead to the formation of a benign neoplasm or "new growth." The initial neoplasm usually appears in an organ as a solid mass. With increasing chromosomal changes, a carcinoma is formed (Muir & Anderson, 1985). A carcinoma is a malignant tumor originating from the epithelia and accounts for over ninety percent of malignant tumors. Tumors are very common, but they usually do not pose any threat to the host because they are small and localized. These tumors are termed benign. The cellular makeup of benign tumors is very similar to normal cells, and their cell-adhesion molecules keep the tumor contained to the original site (Lodish, 2004). Benign tumors are generally encapsulated and slow growing. From the microscopic level, they are usually well differentiated and uniform throughout (Muir & Anderson, 1985). However, a malignant tumor contains cells that grow rapidly. This type of tumor is also known as cancer. Their ability to invade and spread to distant areas differentiates malignant tumors from benign tumors (Lodish, 2004).

Metastasis

Metastasis is the process where primary tumor cells migrate to a different location and form secondary tumors. The tissues most likely to be attacked are those that create growth factors and generate new vasculature. These tissues include bone, blood vessels, and the liver. The process of metastasis can be divided into several steps. First, the individual tumor cells separate from the primary tumor. These malignant cells must

permeate the basement membrane, get through the extracellular matrix, and intravasate into the blood or lymphatic vessels (Howell & Grandis, 2005). Breaking down the basement membrane enables the tumor cells to enter the blood, but only a small percentage survive to form a secondary tumor (Lodish, 2004). From this stage, the cells can migrate to different sites. Before a metastatic tumor is formed, the cells must invade the target organ (Howell & Grandis, 2005). The process requires communication with tumor cells, stromal cells, extracellular matrix, and vasculature mediated by growth factors, cytokines, and enzymes (Miyazaki et al., 2006). Malignant tumors have atypical structure, and they are usually less differentiated. The cells have a loss of polarity and tend to have abnormal mitotic figures (Muir & Anderson, 1985).

Several proteins are involved in making cells capable of invasion and metastasis. Two classes are cell-cell adhesion molecules and integrins. Cell adhesion molecules are found on all cells and provide a connection between the extracellular matrix and cytoskeleton. These molecules are involved in communication between the interior and exterior of the cell and processes such as growth, proliferation, and migration. Integrins are adhesion receptors that are responsible for adhesion to the adjacent matrix (Lyons & Jones, 2007). Cadherins are a part of the intracellular adhesions in normal cells (Kramer, Shen, & Zhou, 2005). As the cells migrate through the extracellular matrix, they change these intracellular adhesions. E-cadherin, which is expressed in epithelial cells, is frequently altered in cancers. This is done by inactivating E-cadherin or ß-catenin genes, repressing the transcriptional activity, or degrading the cadherin extracellular domain. Experiments show that the loss of E-cadherin function is a factor in invasion and metastasis by epithelial

cancers. Carcinomas can also increase their invasion potential by altering integrin expression (Hanahan & Weinberg, 2000). The integrin receptors interacting with the extracellular matrix ligands, in addition to changes in the cadherins, result in cytoskeleton remodeling by Rho family members (Kramer et al., 2005). Extracellular proteases also play a role in invasion and metastasis. Protease gene expression is increased, protease inhibitors are decreased, and zymogen forms of proteases are activated (Hanahan & Weinberg, 2000).

Head and Neck Cancer

Cancer causes approximately one-fifth of the deaths annually in the United States, with 100 to 350 deaths out of every 100,000 people worldwide (Lodish, 2004). Squamous cell carcinoma is the most prevalent form of head and neck cancer. In most cases, cells derived from these tumors are anchorage dependent and usually do not grow in semi-solid cultures. This emphasizes the role of cellular and extracellular matrix interactions (Ziober, Silverman, & Kramer, 2001). Head and neck squamous cell carcinoma (HNSCC) is also the fifth most prevalent form of cancer in the world (Mandal et al., 2008). It involves cancer of the oral cavity, pharynx, and larynx. Overall, only fifty percent of patients diagnosed with head and neck cancer will survive for five years. This survival rate is lower for patients presenting with more advanced cancer and around 4% for patients with stage IV hypopharyngeal lesions (Miyazaki et al., 2006). However, there is an eighty-two percent five-year survival rate for patients with localized oral cancer (*Oral cancer*.2009). The overall low survival rate is due to cancer reoccurrence and local invasion.

Additionally, head and neck cancer is commonly in an advanced stage when it is recognized and treated (Ziober et al., 2001). This form of cancer frequently spreads to the lymph nodes of the neck due to the invasive nature of the cells and the amount of lymphatic drainage from the oral cavity (Kramer et al., 2005). In 2009, it was estimated that there would be 35,720 new cases and 7,600 deaths from oral cancer in the United States (*Oral cancer*.2009).

There are several risk factors for head and neck cancer, the most well known of which is tobacco use, and HNSCC was one of the first tumor types found to have *P53* mutation due to tobacco (Stadler et al., 2008). Men are more likely to have oral cancer than women, because traditionally men abuse alcohol and tobacco for longer periods of time. Oral cancer is more common after age thirty-five, with half the patients diagnosed over age sixty-eight. Of the patients diagnosed with oral cancer, 90% use tobacco, and the likelihood of developing cancer increases with the amount and duration of time the tobacco is used. Additionally, 75 to 80% of patients with oral cancer drink alcohol regularly (*Oral cancer*.2009).

Surgery, radiation therapy, chemotherapy, and newly targeted therapy are the current treatment options for patients with HNSCC (*Oral cancer*.2009). Surgery is the primary form of treatment, but this can have a large effect on the patient's physical appearance (Yeudall et al., 2005). Radiation therapy is frequently used for small cancers, but can be combined with other treatment options for larger cancers. Post-operative radiotherapy is also used to kill remaining cells that have not been removed surgically (*Oral cancer*.2009). Unfortunately, HNSCC does not respond well to radiation or

chemotherapy treatments (Yeudall et al., 2005). One targeted therapy used for HNSCC involves the epidermal growth factor receptor, which is frequently upregulated in this cancer and allows the cells to have resistance against radiation and chemotherapy (*Oral cancer*.2009). Immunotherapy is also emerging as a form of treatment for HNSCC (Rapidis & Wolf, 2009). Since an effective treatment does not exist, early detection and prevention have a large role in preventing death as a result of HNSCC (Yeudall et al., 2005).

Intermediate Filaments

Intermediate filaments are a class of filaments of around 10 nm in diameter making them smaller than microtubules and larger than microfilaments. Microtubules, microfilaments, and intermediate filaments are the main cytoskeletal components in mammalian cells. Intermediate filaments are a part of most differentiated cells and are present in the nucleus and cytoplasm. They are dynamic structures that are constantly reassembling and interacting with the cytoskeleton and cellular organelles (Parry & Steinert, 1995). There are around seventy genes in the human genome encoding different intermediate filaments, and they have been categorized into different types. Type I consists of acidic keratins, and all other keratins (neural and basic) are type II. Keratins are the most numerous and complex intermediate filaments. They cannot form polymers with other intermediate filaments. Keratins are only able to form heteropolymers, because both type I and type II keratins are required for assembly. Desmin, vimentin, periphin, and GFAP (glial filament acidic protein) are all type III intermediate filament proteins. Type III

proteins can form homopolymers and heteropolymers with other proteins in the type III family. Type IV intermediate filament proteins are associated with nerve cells and affect the growth of axons. This type includes a-internexin and neurofilament proteins NF-L, NF-M, and NF-H. These types of intermediate filament proteins are further grouped according to their sequence homology. Group one consists of the keratins. Type III and IV make up group two, while the third group contains the lamins. The primary function for intermediate filament proteins is maintaining the cell and tissue structure. The organization of organelles and proteins inside the cell is also affected by intermediate filaments. Although there is great variety between the different intermediate filaments, they have the same basic structure. There is a central a-helical domain that is surrounded by a non-helical N-terminal ("head") domain and a C-terminal ("tail") domain. The "head" and "tail" domains vary in size and primary amino acid sequence among the different types of intermediate filaments. However, the central domain remains the same throughout the types (Minin & Moldaver, 2008).

Vimentin

Vimentin is a 54 kDa type III intermediate filament that is found in fibroblasts, lymphocytes, endothelial cells, and most mesenchymal tissues. It is also present in a lot of cells during early development. Vimentin filaments combine to create a cytoskeletal network originating at the nucleus and spreading to the plasma membrane throughout the cytoplasm (Paramio, 2006). Vimentin has been shown to move towards the cell surface and the nucleus. It also has the ability to move in multiple directions along the microtubule

due to the motor proteins kinesin and dynein (Minin & Moldaver, 2008). Vimentin interacts with kinesin through a vimentin-associated protein. This interaction causes vimentin to move towards the microtubule plus-ends and the cell surface (Gyoeva & Gelfand, 1991). Vimentin also associates with dynein and dynactin, which are responsible for vimentin moving to the microtubule minus-ends and the cell nucleus (Eriksson et al., 2004). Vimentin expression has been shown in breast cancer cell lines, and there are links between vimentin levels and invasive cervical cancer. The presence of vimentin has been reported in several human epithelial tumors including renal, thyroid, ovarian, and pulmonary carcinomas (Gilles et al., 1996). Vimentin has also been found overexpressed in invasive prostate cancer cells (Singh et al., 2003).

Vimentin Gene Expression

Several transcriptional regulatory elements have been discovered that affect vimentin gene expression. The human vimentin gene has multiple transcription factor binding sites. These sites include "a consensus TATA box, a GC box indispensable for expression and interacting with Sp/XKLF factors, a PEA3 binding site, a NF-?B site, a repressor site, a tandem AP1 binding site, and an anti-silencer element" (Zhou, Kahns, & Nielsen, 2009).

Keratin

Keratins form type I and type II intermediate filaments, and they are found in almost all epithelial cells. They are involved in physiological functions such as maintaining

the cell shape and assembling cell-substrate and cell-cell adhesion sites (Ghosh et al., 2002). Keratins also help protect epithelial cells from stresses that could cause the cells to rupture. Their molecular weights range between 40 to 70 kDa (Gu & Coulombe, 2007), with K13, K14, and K15 around 50 kDa. The gene expression of keratins is developmentally regulated, thus different stages of development are characterized by different keratins. All keratin intermediate filaments include a type I and a type II filament. Additionally, K13, K14, and K15 are all expressed in non-keratinizing stratified squamous epithelia (Chu & Weiss, 2002).

Epithelial to Mesenchymal Transition

The process where epithelial cells become mobile by detaching from their normal junctions and start migrating is known as the epithelial to mesenchymal transition (EMT). EMT is considered a marker of tumor progression indicating invasive and metastatic carcinomas (Voulgari & Pintzas, 2009). Epithelial cells are characterized for being polarized and maintaining tight junction with their neighboring cells, which prevents movement. These cells are normally rich in keratin intermediate filaments, whereas mesenchymal cells do not possess the well-defined intracellular junctions and are motile (Guarino, 2007). These cells typically have a spindle-like structure and exhibit front-to-back polarity, and vimentin is the major intermediate filament present in mesenchymal cells (Hollier, Evans, & Mani, 2009). EMT occurs during many developmental processes including gastrulation, as well as playing a large part in cancer progression. Several steps have defined the process. First, various signaling pathways are modified which determine a

group of cells that will undergo EMT. Next, the intracellular adhesions maintained by cadherins are lost along with the polarity markers. The cell has changes in the cytoskeleton that promote cell delamination, and ultimately, the basement membrane is disassembled (Levayer & Lecuit, 2008). For this reason, EMT is considered an important step leading to metastasis. At the molecular level, EMT is represented by a decrease in E-cadherin and cytokeratins with an increase in the mesenchymal marker vimentin (Lester, Jo, Montel, Takimoto, & Gonias, 2007).

Regulation of Vimentin

The stability, structure, and assembly of intermediate filament polymers can be regulated by phosphorylation. Phosphorylation of intermediate filaments can also mediate interactions with other intermediate filament associated proteins and affect some tissue-specific structural roles (Liao & Omary, 1996). One study showed that the assembly-disassembly balance of vimentin by phosphorylation could regulate activation of RhoA-binding kinase a (Goto et al., 1998). A high constitutive protein phosphatase activity is paired with intermediate filaments, which implies these proteins have a larger phosphate turnover (Eriksson et al., 1992). With multiple high phosphorylation turnover sites on vimentin, PKA and PKC appear as the most likely regulatory kinases. By increasing phosphorylation at the sites mediated by PKA, there is disassembly into tetrameric subunits. The balance between vimentin polymers and depolymerized subunits and the turnover is regulated by kinase-phosphatase equilibrium. This is regulated by reversible phosphorylation at sites in the N-terminal part of vimentin. However, if Ser-38 and Ser-72

were mutated, PKA-mediated phosphorylation of vimentin was decreased *in vitro* and disassembly was affected. Since some phosphorylation remained, this proved that other sites were still being phosphorylated by PKA. This suggests that all of the PKA sites play a role in the assembly state of vimentin (Eriksson et al., 2004).

Protein phosphorylation also plays a role in regulating integrins in motile cells. PKC is one serine/threonine kinase that regulates integrins, and this affects adhesion and migration (Woods, White, Caswell, & Norman, 2004). PKCe is responsible for a part of the endocytic pathway that allows integrin recycling to the plasma membrane. Without PKCe, fibroblasts decrease movement, and there is an emergence of ß1 integrin/PKCe-containing vesicular structures, which resemble a transient recycling compartment. Research showed that vimentin was targeted for phosphorylation by PKCe in these integrin intracellular vesicles, and this phosphorylation controls the integrins exiting this compartment to the plasma membrane. When PKCe is inhibited, there is a decrease in acidic vimentin and a decrease in serine phosphorylation (Ivaska, Whelan, Watson, & Parker, 2002). It is likely that PKCe and vimentin are released from the vesicles as a complex. An experimental release assay showed Ser6 phosphorylation combined with the other serine residues in the amino-terminal of the PKC mediated cluster of vimentin had a positive effect. Further experiments showed that vimentin influences the migration of cells in a PKCe dependent manner because of the increase in migration seen in PKCe re-expressing cells compared to PKCe null cells. An additional experiment mutated serine residues to alanine to analyze the importance of the N-terminus and the other PKC-sites on vimentin induced cell motility. The researchers also substituted the serines (S4, 6, 7, 8, 9)

with aspartate, which are negatively charged residues and mimic PKCe phosphorylation. The alanine mutation, which is unphosphorylatable, prevented motility, while the aspartate mutation restored motility. The alanine mutation interfered with vimentin filament assembly and caused a buildup of integrin and PKCe positive vesicles comparable to results when PKC activity is inhibited. This showed that PKCe mediated phosphorylation at the N-terminus of vimentin plays a large role in PKCe dependent, vimentin induced cell motility. The mutant vimentin caused decreased recycling of integrins as well, which implies that endocytosed integrin/PKCe containing vesicles link with vimentin. These integrins exit and recycle to the plasma membrane from this vesicle dependent on PKC-mediated phosphorylation of vimentin (Ivaska et al., 2005).

Another phosphorylation site identified on vimentin is Ser-72. Intermediate filament bridges are very common when there are mutations in Rho-kinase, PKC phosphorylation sites, and Ser-72. Of these three, mutation of vimentin at Ser-72 is the most critical mutation site. Experiments demonstrated that phosphorylation of vimentin at Ser-72 was not present in Aurora-B (K/R)- expressing cells, which implied that phosphorylation of vimentin at Ser-72 is controlled by Aurora-B. This phosphorylation by Aurora-B could be involved in segregation of vimentin filaments during cytokinesis. It was also suggested that cleavage furrow-specific intermediate filament phosphorylation could be mediated by both Rho-kinase and Aurora B (Goto et al., 2003).

Nuclear Factor-?B (NF-?B)

NF-?B is a transcription factor widely recognized to be involved in carcinogenesis and control of the immune and inflammatory responses. NF-?B regulates a variety of target genes that are involved in cell proliferation, regulating apoptosis, facilitating angiogenesis, and inducing invasion and metastasis. It has a conserved 300 amino acid Rel homology domain in the N-terminus. This domain is involved in DNA binding, dimerization, and interacting with I?B proteins, which are inhibitory factors (Lee, Jeon, Kim, & Song, 2007). Inactive NF-?B proteins are prevalent in most cells, and they are contained in the cytoplasm in a complex with I?B. I?B kinase is involved in all of the extracellular signals that activate NF-?B. When activated by DNA damage, cytokines, or growth factor signaling, I?B kinase phosphorylates serine residues on I?B (Loercher et al., 2004). Next, I?B is ubiquitinated and degraded by a proteasome, and NF-?B is exposed to nuclear-localization signals. This allows NF-?B to translocate to the nucleus and initiate transcription of a variety of target genes. Ultimately, the NF-?B signaling is stopped by a negative feedback loop. One of the genes NF-?B transcribes is I?B, so the level of I?B increases and binds with NF-?B in the nucleus, and the complex migrates back to the cytosol (Lodish, 2004). This is called the classical or canonical pathway and is triggered by infection or proinflammatory cytokines. The classical pathway is important for innate immunity and inhibiting apoptosis. The alternative or non-canonical pathway is initiated by members from the TNF cytokine family to activate IKKa homodimers by NF-?B-inducing kinase. This pathway is a part of secondary lymphoid organ development and the

adaptive immune response. The atypical pathway does not require I?B and is initiated by UV radiation that damages DNA or doxorubicin (Lee et al., 2007).

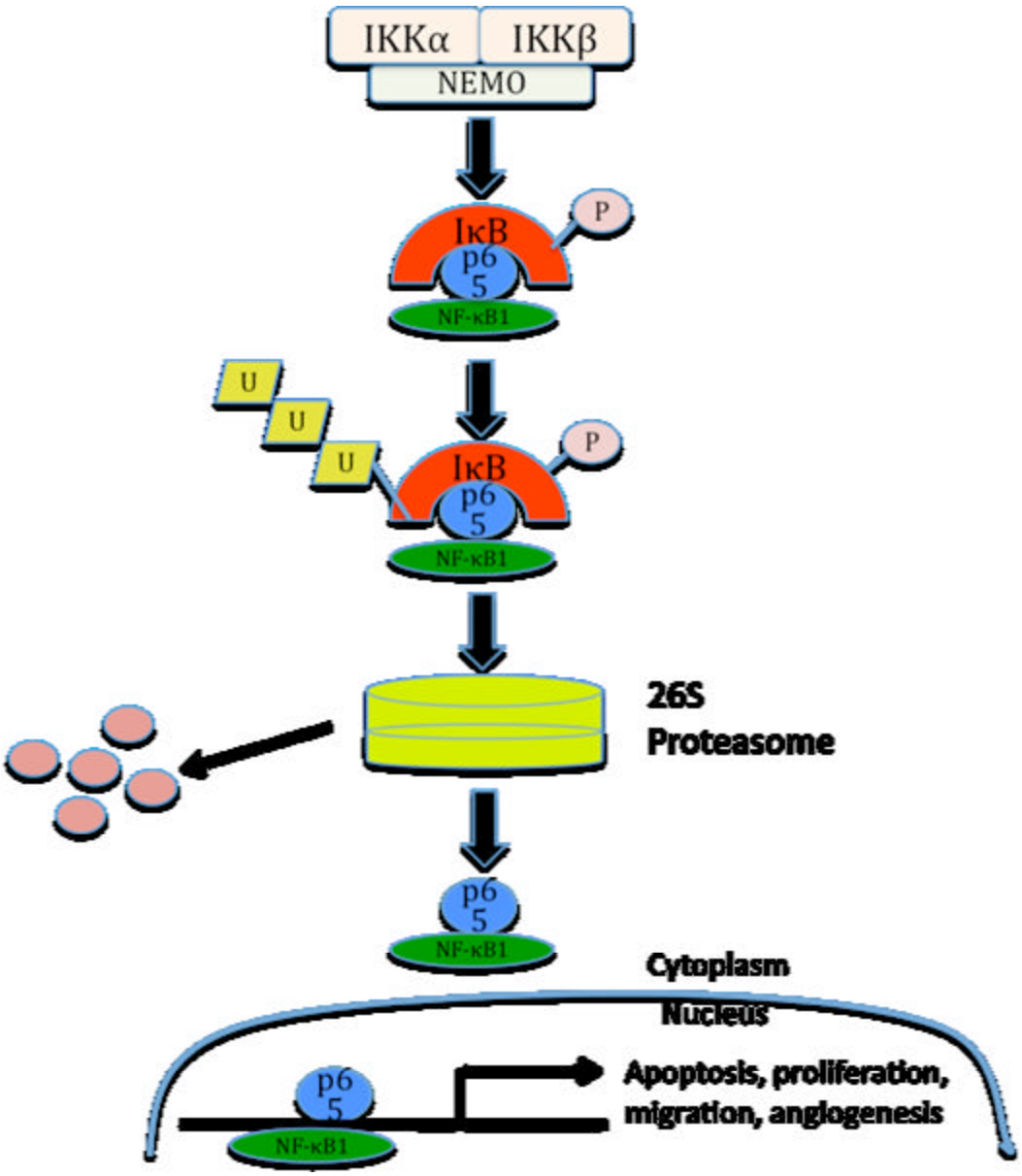


Figure 1: The canonical NF-?B signaling pathway.

Nuclear Factor-?B (NF-?B) – Involvement in Cancer

NF-?B is capable of inducing several of the six hallmarks of cancer and has also been found constitutively activated in some cancer cells. This activation could result from several mechanisms. Viral onco-proteins are capable of constitutively activating NF-?B. Changes such as translocations, deletions, and mutations potentially interrupt the genes that regulate activation causing constant NF-?B activation. Proinflammatory cytokines stimulated by autocrine or paracrine feedback, as well as activation of signaling molecules can stimulate I?B activity resulting in constitutive activation of NF-?B. Supporting cancer cell proliferation, avoiding apoptosis, and amplifying tumor angiogenic and metastatic potential are all results of constitutively activated NF-?B transcription factors. NF-?B regulates cell proliferation by activating target genes that control growth factors and promote proliferation of lymphoid and myeloid cells. NF-?B is also linked to cyclin D1 (Karin, Cao, Greten, & Li, 2002). Cyclin D1 is a G1 specific cyclin, which promotes progression through the restriction point during the G1 phase of the cell cycle (Kim & Diehl, 2009). There is a NF-?B site in the cyclin D1 promoter, and this initiation of cyclin D1 supports the proliferation of mammary epithelial cells throughout pregnancy (Karin et al., 2002). There is overexpression of cyclin D1 in about 80% of HNSCC. Experiments show that inhibiting NF-?B results in decreased cell cycle progression, and this can be reversed by transfection and expression of a cyclin D1 plasmid (Allen, Ricker, Chen, & Van Waes, 2007). NF-?B is also able to inhibit apoptosis. Several anti-apoptotic factors induced by NF-?B include caspase-8/FADD (FAS-associated death domain)-like IL-1ß converting enzyme (FLICE) inhibitory protein (cFLIP) and members of the BCL2 family.

Constitutively activated NF-?B stops the apoptotic response to anticancer drugs and radiation. NF-?B anti-apoptotic effects can facilitate the formation of neoplasms by making cells that have had chromosomal rearrangements or other DNA damage more resistant to cell death. Additionally, chemokines play an important role in angiogenesis, and cells with increased levels of NF-?B have elevated production of some proangiogenic chemokines. This results in greater migratory activity. IL-8 is a chemokine regulated by NF-?B that is involved in enhancing angiogenesis (Karin et al., 2002). It has a NF-?B binding site in its promoter, which is elevated in patients with HNSCC (Allen et al., 2007). Also, activation of NF-?B plays a role in destruction of the extracellular matrix by cancer cells (Karin et al., 2002). Blocking NF-?B activity has shown decreased angiogenesis, invasion, and metastasis (Lee et al., 2007). Furthermore, matrix metalloprotease-9 (MMP-9) is commonly overexpressed in HNSCC. MMP-9 requires NF-?B for expression, and higher levels of MMP-9 are associated with nodal metastasis. Furthermore, cigarette smoke condensate causes NF-?B activation by phosphorylation and degradation of I?B, which is consistent with why smoking is a risk factor for HNSCC (Allen et al., 2007).

Since NF-?B plays a role in inhibiting apoptosis and promoting tumor progression and is found constitutively activated in many cancers, NF-?B inhibitors could be useful in cancer therapy. However, NF-?B inhibitors are not very specific and inhibit other necessary signaling systems. Since NF-?B is activated by a variety of pathways, the likelihood of a single inhibitor to affect all tumors is low (Lee et al., 2007). Current inhibitors target the proteosome, I?B, and kinases upstream with a role in NF-?B activation. Clinical and preclinical studies have shown anticancer activity with these

agents. Bortezomib (PS-341) inhibits the proteasome and has improved results with radiation in metastatic HNSCC (Ferris & Grandis, 2007). This drug has shown decreased expression of cyclin D1, Bcl-XL, and IAP-1, which are all regulated by NF-?B in HNSCC (Allen et al., 2007). Inhibition of NF-?B has been shown to stop proliferation, cell survival, migration, angiogenesis, and tumorigenesis. All of this suggests that NF-?B modifies the gene expression profile and malignant phenotype (Loercher et al., 2004).

Wnt-dependent Signaling Pathway

The Wnt-dependent signaling pathways consist of three molecular pathways downstream of the Wnt/Frizzled (Fzd) interaction. The "canonical" Wnt pathway involves Wnt and ß-catenin. The "non-canonical" pathways consist of Wnt/$Ca^{2+}$ and Wnt/polarity.

| **Wnt Pathway** | **Wnt Ligands for Activation** |
|---|---|
| Wnt/ß-catenin - "canonical" | Wnt 1, 3A, 8 and 8B |
| Wnt/$Ca^{2+}$ - "non canonical" | Wnt 4, 5A, and 11 |
| Wnt/polarity - "non canonical" | Wnt 4, 5A, and 11 |

Table 1: Wnt Pathways and Wnt Ligands for Activation

Although each pathway is different, they share the same initial step of the Wnt ligand binding to the appropriate Fzd receptor. The Fzd receptor is a seven pass transmembrane receptor. The human genome contains nineteen Wnt ligands and ten different members of the Fzd seven-transmembrane receptor family. There are four

families of Wnt antagonists that have been assigned to two groups based on their mode of action. Secreted Frizzled related protein (sFRP) family, Wnt inhibitory factor-1 (WIF-1) and Cerberus are the first group. This group inhibits Wnt signaling by directly binding to the Wnt molecules. The Dickkopf (DKK) family makes up the second group, and they inhibit Wnt signaling by binding to the LRP5/LRP6 component of the Wnt receptor complex (Janssens, Janicot, & Perera, 2006). The Wnt signaling pathway is involved in several important developmental events, including brain development, limb patterning, and organogenesis. This pathway also regulates formation of osteoblasts and controls stem cells. Interruptions in this signaling pathway are found in multiple cancers (Lodish, 2004).

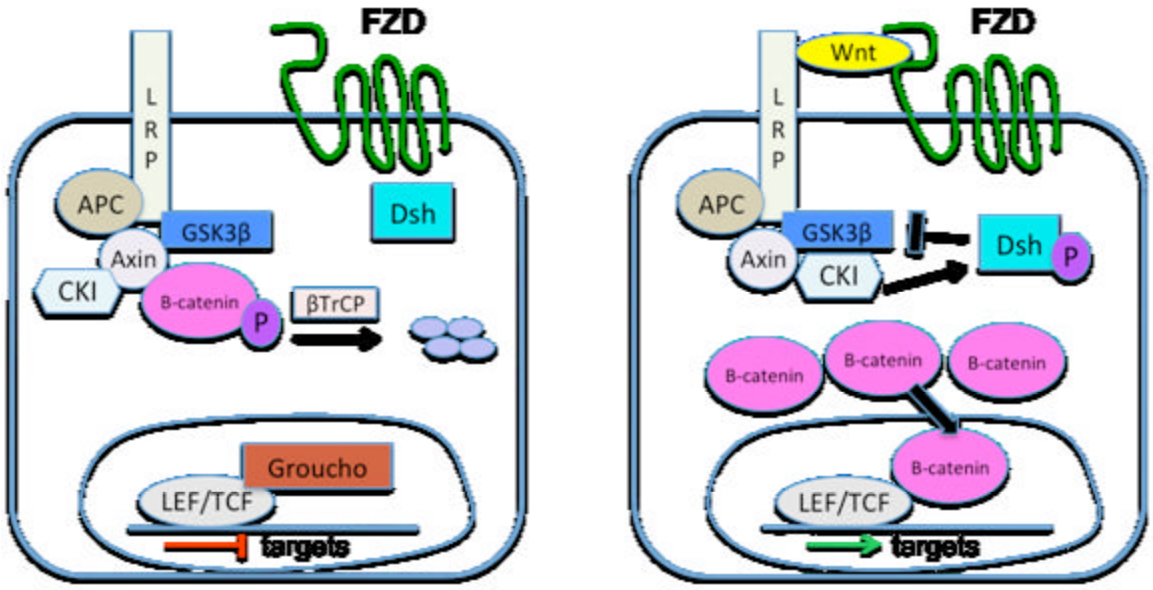


Figure 2: The Wnt/ß-catenin signaling pathway. (Left) A schematic showing the absence of a Wnt ligand. (Right) A schematic showing the presence of a Wnt ligand.

ß-catenin, a cytoplasmic protein, is the central molecule in the Wnt/ß-catenin pathway. This pathway affects several cellular processes including cell adhesion, growth, and differentiation (Du et al., 2009). For this pathway, an additional single-pass transmembrane protein from the low-density lipoprotein receptor family (LRP5 or LRP6) serves as a co-receptor of the seven transmembrane Fzd receptors to conduct the Wnt signal. Activation of the pathway begins with Wnt binding to the receptor complex consisting of the Fzd receptor and LRP co-receptor (Janssens et al., 2006). Wnt signaling inhibits the multi-protein ß-catenin degradation complex. This complex is formed by the scaffold protein axin, the serine/threonine kinase glycogen synthase kinase 3ß (GSK3ß), the tumor suppressor protein APC, and ß-catenin (Kühl, 2003). Once Wnt is bound, dishevelled (Dvl) is phosphorylated, and its relationship with axin inhibits GSK3ß and casein kinase 1a (CK1a) from phosphorylating important substrates such as ß-catenin. Phosphorylation of ß-catenin is required for its degradation. Without phosphorylation, ß-catenin localizes to the nucleus, forms a complex with TCF/LEF (T-cell factor/lymphoid enhancer factor) transcription factors and other co-activators that allow expression of downstream target genes. When the Wnt/Fzd signal is not present, GSK3ß and CK1a phosphorylate ß-catenin, which targets it for degradation. Thus, ß-catenin will not collect in the nucleus, so TCF/LEF proteins serve as transcriptional repressors (Janssens et al., 2006).

Multiple studies have shown that abnormal Wnt/ß-catenin signaling is involved in human cancer. In colon cancer, a mutation in APC causes ß-catenin to buildup in the cytoplasm and enter the nucleus. This causes increased proliferation and carcinogenesis by

ß-catenin interacting with TCF-4/LEF (Du et al., 2009). A transgenic mouse model has suggested that Wnt-1 expression supports tumor growth, and there is evidence in human breast cancer showing Wnt signaling promotes tumor development. When Wnt1 is expressed, cells are resistant to cancer therapies based on apoptosis by inhibiting ß-catenin/TCF mediated transcription. Studies have shown advantages for blocking Wnt signaling in cancer patients, because inhibiting the Wnt/ß-catenin signaling pathways allows apoptosis and chemotherapy to work more effectively (Janssens et al., 2006). The Wnt/ß-catenin pathway has also been shown to regulate the transcription factor Twist in mouse mammary epithelial cell lines and tumors. Twist and Wnt1 can both inhibit lactogenic differentiation, which possibly causes mammary tumorigenesis (Howe, Watanabe, Leonard, & Brown, 2003). Wnt5a is involved in cell motility and invasion in metastatic melanoma, because when its receptor is blocked, PKC activity and cellular invasion are inhibited (Janssens et al., 2006). Wnt5a has been classified as a gene more prevalent in highly aggressive tumors compared to less aggressive tumors. This member of the Wnt family is independent of ß-catenin and acts through the non-canonical Wnt signaling pathway by binding a G-protein-coupled receptor to activate PKC and intracellular calcium. Increasing Wnt5a in melanoma cells resulted in increased PKC activation and motility and poor patient outcome. Wnt5a increases vimentin expression and decreases E-cadherin. Experiments demonstrated Wnt5a could increase metastatic melanoma through initiating EMT in a PKC-dependent manner (Dissanayake et al., 2007).

ß-catenin

In normal epithelial cells, ß-catenin is found in complexes with E-cadherin and plays a part in cell-cell adhesion. ß-catenin is also found accumulating in the cytoplasm or translocating to the nucleus. Both of these locations are associated with epithelial cell migration and EMT. Several genes are targeted by ß-catenin/TCF transcription, including MMP-7, c-myc, and cyclin D1 (Gilles et al., 2003). The ß-catenin promoter includes NF-?B DNA binding motifs (Loercher et al., 2004). ß-catenin can act as an oncoprotein in several cancers, and mutations in the region of the gene encoding the amino terminal of ß-catenin can affect the serine and threonine residues involved in phosphorylation by GSK3ß and CK1 that label ß-catenin for degradation. Both APC and axin are important for down-regulation of ß-catenin (Janssens et al., 2006). Crosstalk also exists in bacterial-colonized HCT116 intestinal epithelial cells between NF-?B and ß-catenin. Constitutively expressed ß-catenin stabilizes I?Ba indirectly which results in NF-?B inhibition (Du et al., 2009). Vimentin expressing cells have a larger amount of ß-catenin/TCF transcriptional activity than vimentin-negative cells, and experiments support vimentin as a target of the ß-catenin/TCF pathway. The human vimentin promoter is reported to contain a ß-catenin/TCF binding site 468 bp upstream of the transcriptional start site. In mammary human epithelial cell lines, the localization of ß-catenin in the cytoplasm and nucleus is associated with vimentin expression and is restricted to invasive or migrating cells (Gilles et al., 2003).

The Dickkopf Family

The Dickkopf family consists of secreted proteins ranging in size from 255 to 350 amino acids, and there are four main forms found in vertebrates. DKK-1 and DKK-4 are pure Wnt/ß-catenin inhibitors. DKK-2 and DKK-3 can activate or inhibit the Wnt/ß-catenin pathway depending on the cellular context. Members of the DKK family inhibit through two mechanisms. The first mechanism involves DKK directly binding to LRP5/6 and blocking the Wnt-LRP interaction. The second mechanism requires the DKK family member forming a complex with LRP5/6 and the DKK receptor Kremen. This complex causes endocytosis, and LRP5/6 is removed from the plasma membrane, which inhibits the Wnt/ß-catenin pathway (Pendas-Franco, Aguilera, Pereira, Gonzalez-Sancho, & Munoz, 2008).

Dickkopf-3 (DKK-3)

DKK-3 is found on chromosome 11p15, and this region is a significant target of methylation-mediated genetic imprinting (Yu et al., 2009). High levels of DKK-3 have been found in tumor endothelial cells of glioma, high-grade non-Hodgkin's lymphomas, melanoma, and colorectal cancers. Additionally, DKK-3 is a potential marker during tumor angiogenesis for endothelial cell activation (Pendas-Franco et al., 2008). DKK-3 is a strong regulator of cell invasion, but can be transcriptionally inhibited in a membrane type-1-MMP (MT1-MMP) dependent manner. This member of the DKK family serves as a tumor suppressor by halting cell growth and motility. In urothelial cell carcinoma, DKK-3 assists

inhibition of the Wnt signaling pathway, which results in tumor suppression (Saeb-Parsy et al., 2008). The absence of DKK-3 can allow activation of the Wnt signaling pathway and support tumor growth through disregulation of cell proliferation and differentiation. It is possible that down-regulation of DKK-3 in various cancers occurs as a result of promoter methylation. This is the common reason for decreased DKK-3 expression in gastric and colon cancers, and DKK-3 is often reduced or silenced in gastric and colon cancer cell lines (Yu et al., 2009). Methylation of the DKK-3 promoter in primary gastric cancer was associated with poor patient outcome. Studies showed that the decreased expression of DKK-3 in colon cancer cells is caused by promoter methylation. DNA-methyltransferase activity inhibited by 5-aza-2'-deoxycytidine (5-Aza-dC) reversed the methylation, and the silenced gene was re-expressed. There was an increase in DKK-3 mRNA expression in the silenced cell lines once treated with 5-Aza-dC supporting that methylation was the major cause of decreased DKK-3 expression in digestive cancer cells. Constant expression of DKK-3 results in decreased colony formation. This inhibition by DKK-3 on cell growth has also been shown in lung cancer and osteosarcoma cells (Yu et al., 2009).

Previous Research in Our Lab

Previous research in our lab has shown that HN12 cells, derived from a lymph node metastasis, express a higher level of vimentin than HN4 cells, derived from a primary tumor on the tongue. HN12 cells also have decreased expression of several keratins, including K13, K14, and K15. RNA interference was used to inhibit vimentin expression in HN12 cells to determine the effects of vimentin overexpression, and this inhibition

resulted in decreased proliferation, migration, and invasion. Additionally, these vimentin knockdowns showed an up-regulation of K13, K14, and K15. In athymic mice, these cells showed smaller and more differentiated tumors. Through quantitative PCR and promoter assays, the data showed that the re-expression of these keratins in the vimentin knockdown cells was a result of increased transcription (Paccione et al., 2008).

Additional studies in our lab have demonstrated that DKK3, a Wnt antagonist, is inhibited by promoter methylation in HN12 cells. With 5-aza-2'-deoxycytidine, this inhibition is relieved, and there are decreased levels of ß-catenin transcriptional targets. Other studies have shown that ß-catenin increases vimentin expression through Wnt signaling (Gilles et al., 2003). This suggests that by inhibiting DKK3, Wnt signaling could increase vimentin expression, and this could cause decreased keratin expression. Currently, the mechanism for the repression of keratins in the presence of vimentin overexpression is unknown.

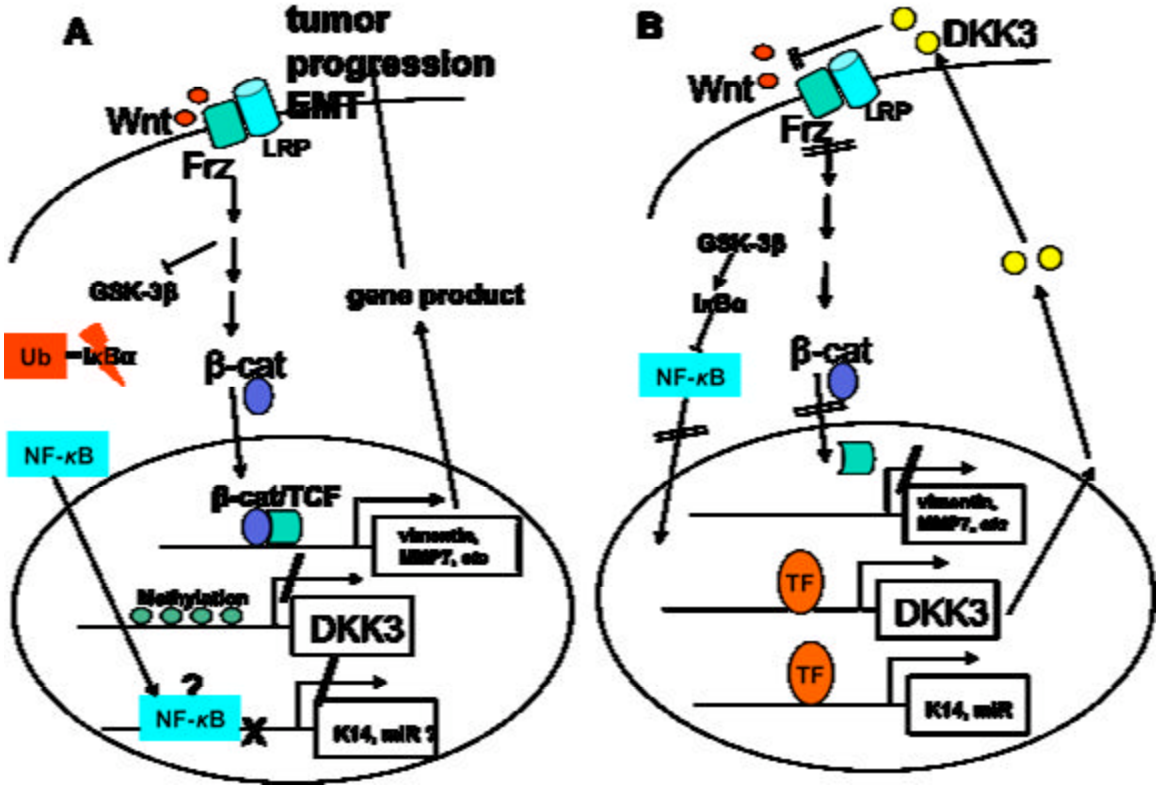


Figure 3: A. DKK3 promoter is methylated and transcription is inhibited. B. DKK3 is expressed which blocks the Wnt signaling pathway.

Hypothesis

The downregulation of differentiation-specific keratins contributes to tumor progression, mediated directly or indirectly by expression of vimentin.

Aims of the Current Study

- To determine keratin gene expression and biological response in cells that express wild-type and PKC phosphorylation site mutants of vimentin

- Vimentin will be expressed in vimentin-negative tumor cells and expression of K14 will be determined by western blot and qPCR.
- Proliferation rate will be determined by cell counting.
- Effects on cell motility and invasion will be determined by wound-closure assays.

- To determine the role of Wnt signaling in vimentin expression during EMT.
  - Determine the effect of NF?B inhibitor on HN12 cell growth.
  - Determine the effect of 5-Aza-C on HN12 cell growth.
  - Proliferation will be determined by cell counting.
  - 5-azaC will be used to relieve the repression on the DKK3 promoter in cells where it is repressed by methylation.
  - Vimentin expression will be determined.

## Methods

### Cell Culture

HN4 cells were obtained from a primary squamous cell carcinoma of the tongue. HN12 cells were obtained from a nodal metastasis in the same patient. HNSCC cells lines were cultured in Dulbecco's Modification of Eagle's Medium (DMEM) containing 10% fetal bovine serum (FBS), penicillin-streptomycin (10$\mu$g/ml), and L-glutamine (10$\mu$g/ml). All cells were maintained at 37°C in 90% air/10% $CO_2$.

### Growth Factors and Inhibitors

HN4 cells expressing the vimentin mutations generated by transfection were cultured as above in the presence of G418 (400$\mu$g/mL). HN4 shDKK3 cells were cultured in DMEM in the presence of puromycin (1$\mu$g/ml). NF-?B inhibitor was prepared in DMSO as a stock solution of 2mM. 5-Aza-dC was prepared in PBS as a stock solution of 6mM.

### Plasmids

The plasmids pCMV Vim-Wt, pCMV Vim-Ala, and pCMV Vim-Asp encode amino acid substitutions at serines 4,6,7,8,9. In pCMV Vim-Ala, these serine residues have been mutated to alanine, and pCMV Vim-Asp has these serine residues have been mutated to aspartate. These plasmids have been described previously (Ivaska et al., 2005).

Bacterial Transformation

The plasmids pCMV Vim-Wt, pCMV Vim-Ala, and pCMV Vim-Asp were supplied on filter paper. 100 $\mu$L of 1 x TE buffer was added to each plasmid and briefly vortexed. These were stored at 4°C overnight. For bacterial transformation, the plasmids were centrifuged for 2 min at 15.4 rpm, and the competent *E. coli* cells were thawed on ice for 10 min. 5$\mu$l of each sample was combined with 50$\mu$l of competent cells (Bioline, Randolph, MA). 1$\mu$l of the control pUC19 (Bioline, Randolph, MA) was added to the competent cells. Samples were placed on ice for 30 min, then heat shocked at 42°C for 45 s, and immediately placed on ice for 2 min. 250$\mu$l of SOC was added to each tube, and samples were placed in the shaker at 37°C for 1 h. The entire sample was added to an agar plate containing kanamycin (50$\mu$g/mL), then spread using glass beads. The plates were incubated for 15 min at room temperature, and then incubated overnight at 37°C.

Isolating Colonies and Establishing Liquid Cultures

Colonies were picked from the plates after incubating overnight. A single colony was combined with 3mL of 2 x YT medium in a 15mL tube and shaken overnight at 37°C.

Small Scale DNA Preparations

Small scale DNA preparations (Minipreps) were carried out using the Promega Wizard Plus SV Miniprep DNA Purification System (Promega, Madison, WI). This isolated the plasmid DNA from the transformed *E. coli*. Initially, 1.5 mL of the bacterial

culture was centrifuged at 10,000 x g for 5 min. The supernatant was poured off, and 250 $\mu$L of Cell Resuspension Solution was added to resuspend the pellet. The solution was briefly vortexed. Next, 250 $\mu$L of Cell Lysis Solution was added to each sample and mixed by inverting the tube 4 times. Samples were incubated at room temperature for 5 min. 10 $\mu$L of Alkaline Protease Solution was added to each sample and mixed by inverting the tube 4 times. The samples were incubated at room temperature for another 5 min. 350 $\mu$L of Neutralization Solution was added and immediately inverted 4 times to mix. The samples were centrifuged at 14,000 x g for 10 min. The cleared lysate was transferred to a spin column by decanting to avoid transfer of the white precipitate. The supernatant was centrifuged for 1 min at 14,000 x g. The spin column was removed from the tube, and the flowthrough was discarded from the collection tube. Next, the spin column was placed back in the collection tube. 750 $\mu$L of Column Wash Solution was added to each spin column and centrifuged for 1 min at 14,000 x g. The flowthrough was discarded as before, and the procedure was repeated with 250 $\mu$L of Column Wash Solution. The samples were spun for 2 min at 14,000 x g, then the spin column was transferred to a new, sterile 1.5 mL microcentrifuge tube. The plasmid DNA was eluted by adding 100 $\mu$L of Nuclease-Free Water to the spin column and centrifuged at 14,000 x g for 1 min. The spin column was discarded, and the eluted DNA was stored at 4°C.

Larger Scale DNA Preparations

Larger scale DNA preparations (Midipreps) were carried out using the Promega Wizard Plus Midiprep DNA Purification System (Promega, Madison, WI). This isolated the plasmid DNA from the transformed *E. coli*. The cells were centrifuged at 10,000 x g for 10 min at 4°C to form a pellet. The pellet was resuspended with 3mL of Cell Resuspension Solution. Next, 3mL of Cell Lysis Solution was added to each sample and inverted to mix, followed by 3mL of Neutralization Solution and inverted. The samples were centrifuged at 14,000 x g for 15 min at 4°C, and the supernatant containing the DNA was decanted. The resin was reuspended by adding 10mL of resin to the DNA and mixed by swirling. Next, the midicolumn was connected to the vacuum manifold. The resin/DNA mixture was transferred to the midicolumn, and the vacuum was applied. The vacuum was released once all of the liquid passed through the column. 15mL of Column Wash Solution was added to each sample, and the vacuum was applied. This washing step was repeated, and once all of the liquid passed through the column, the vacuum was left on for an additional 30 s. The midicolumn was removed from the vacuum and placed in a 1.5mL microcentrifuge tube, where it was centrifuged for 2 min at 10,000 x g. After being spun down, the midicolumn was transferred to a new microcentrifuge tube, and 300$\mu$L of preheated water was added to each sample. The samples incubated for 1 min and were centrifuged at 10,000 x g for 20 s to elute the DNA. The elutate was centrifuged for 5 min at 10,000 x g to pellet the resin fine. The supernatant that contained the DNA was transferred to a new microcentrifuge tube and stored at -20°C.

Nuclear Transfection

The pCMV Vim-Wt, pCMV Vim-Ala, and pCMV Vim-Asp plasmids were transfected into HN4 cells using the Lonza Nucleofector Kit (Lonza Inc., Gaithersburg, MD) using 4 $\mu$g of midiprep DNA. HN4 cells were trypsinized, counted, and distributed into four tubes (2 x $10^6$ cells per tube). Each tube was centrifuged, and the medium was aspirated. The cell pellet was resuspended with 100 $\mu$L of Nucleofector Solution and transferred to a cuvette. 4$\mu$g of plasmid DNA and 0.5$\mu$g GFP plasmid were added to each cuvette. The cuvette was inserted into the Nucleofector, and the cells were transfected using program T-20. Once the transfection was complete, the cuvette was removed from the machine, and 500 $\mu$L of warm medium with serum was added. This suspension was transferred to a 10 mm plate containing 10 mL of complete growth medium. The GFP plasmid was added to serve as an internal control for transfection efficiency.

Transient Transfection

The pCMV Vim-Wt, pCMV Vim-Ala, pCMV Vim-Asp plasmids and GFP, as a control, were transfected into 293T cells to confirm expression. 5 x $10^4$ cells were plated per well in a 6-well plate for 24 h in complete growth medium. In a sterile microcentrifuge tube, 3 $\mu$L/$\mu$g of Trans IT-Keratinocyte Transfection Reagent (Mirus, Madison, WI) was added dropwise into 200 $\mu$L of serum-free medium and mixed by vortexing. This solution was incubated for 20 min at room temperature. 2 $\mu$g of DNA was added to the diluted Trans IT-Keratinocyte Reagent and mixed by gentle pipetting. This solution was again incubated for 20 min at room temperature. Next, the medium was removed from the 293T

cells and replaced with 2 mL per well of fresh complete growth medium. The Trans IT-Keratinocyte Reagent/DNA complex mixture was added dropwise to the 293T cells. The plate was gently rocked to evenly distribute the mixture in the wells and incubated at 37°C for 48 h.

Western Blot

Total cellular protein extracts were prepared as follows. Cells were washed with cold PBS two times, and then 50$\mu$L of vimentin lysis buffer was added to each well. After incubating 10 min on ice, the samples were collected and centrifuged for 10 min at 4°C and 10.4 rpm. 12.5 $\mu$L of 5 x SDS-PAGE buffer was added to each sample. The samples were heated for 10 min at 100°C, and then placed on ice for 2 min. The lysates were resolved by 10% SDS-polyacrylamide gel (Sambrook & Russell, 2001) electrophoretically at 120 V in 1 x SDS-PAGE running buffer. Fractionated proteins were transferred to PVDF membranes (Immobilon-P, Millipore Corporation, Bedford, MA) overnight in 1 x transfer buffer. The membranes were blocked in 5% non-fat dried milk in 0.05% Tween-TBS (T-TBS) for 1 h at room temperature, washed three times for 5 min with 0.05% T-TBS, and incubated overnight with the primary antibody on a shaker at 4°C. Next, the membranes were washed three times with TTBS for 5 mins. After washing, the membranes were incubated with HRP-conjugated secondary antibodies at room temperature for 1 h. The membranes were washed again with TTBS three times for 5 min. Finally, the membranes were incubated at room temperature for 2 min with Western Lightning

Chemiluminescence Reagent Plus (Perkin Elmer Life Sciences Inc., Boston, MA) and imaged using Kodak film.

| Primary Antibody | Supplier | Dilution |
|---|---|---|
| Vimentin | Sigma, St. Louis, MO | 1:5000 |
| Keratin 14 (hybridoma supernatent) | Gift of Dr. A. Waseem, University of London | 1:1000 |
| Actin | Santa Cruz Biotechnology, Santa Cruz, CA | 1:1000 |
| DKK3 | Abcam, Cambridge, MA | 1:500 |

Table 2: Primary Antibodies for Western Blotting

Immunofluorescence

Cells (5 x $10^3$) were plated on coverslips in 12-well plates and allowed to grow until 75% confluent. Cells were washed with PBS, and then fixed in cold methanol for 20 min. The cells were permeabilized in PBST (PBS and Triton X) for 5 min, and then blocked in 5% BSA in PBST for 1 h at room temperature. Cells were incubated with the primary antibody diluted in blocking buffer overnight at 4°C. The cells were washed six times for 5 min with PBST and incubated with a FITC-conjugated secondary antibody at a 1:500 dilution in blocking buffer and 1$\mu$g/mL DAPI for 1 h at room temperature. The coverslips were mounted on a microscope slide with Vectashield and analyzed with a Zeiss Axiovert 200 inverted fluorescence microscope.

| Primary Antibody | Supplier | Dilution |
|---|---|---|
| Vimentin | Sigma, St. Louis, MO | 1:500 |
| Keratin 14 (hybridoma supernatent) | Gift of Dr. A. Waseem, University of London | 1:250 |
| ?-catenin | Santa Cruz Biotechnology, Santa Cruz, CA | 1:100-1:200 |
| E-cadherin | Sigma, St. Louis, MO | 1:100-1:200 |

Table 3: Primary Antibodies for Immunofluorescence

MTT Assay

Cells were plated at $5x10^3$ cells per well in a 12-well plate in triplicate and allowed to grow to 80% confluence. 100 $\mu$L of MTT reagent (3-(4,5-Dimethylthiazolyl-2)-2,5-Diphenyl Tetrazolium Bromide in PBS) (MP Biomedicals Inc., Solon, OH) was added to each well, and the cells incubated for 4 h at 37°C in 90% air/10% $CO_2$. The medium and reagent were removed from each well, and the formazan crystals were solubilized in 1 mL of MTT solubilization buffer (0.01M HCl with 10% SDS) per well and incubated overnight. Absorbance was measured spectrophotometrically at 570 nm. The MTT solubilization buffer was used as the blank measurement.

Cell Proliferation Assay

Cells were plated at 5 x $10^3$ cell per well in 6-well plates. They were cultured for three days before counting and counted for five consecutive days using a hemacytometer. Each cell line was plated in triplicate, and each well was counted twice. For counting, the cells were trypsinized with 250 $\mu$L trypsin and incubated until all of the cells were detached. The trypsin-cell suspension was neutralized with 1 mL of medium and centrifuged at 1.0 rpm for 5 min. Cells were resuspended in 0.1 mL, 0.5 mL, or 1 mL of medium and counted.

RNA Extraction

Cells were plated in 6-well plates and allowed to grow until they were 75% confluent. The medium was removed, and 1 mL of Trizol reagent (Life Technologies, Carlsbad, CA) was added to each well. The plate was incubated for 5 min on a shaker. After incubating, the entire contents of the well were transferred to a microcentrifuge tube and incubated for 2 min, then 200 $\mu$L of chloroform was added to each tube. The tubes were shaken vigorously by hand, and then centrifuged at 4°C for 15 min at 12,000 x g. The clear aqueous phase was carefully pipetted to a new microcentrifuge tube. 0.5 mL of isopropyl alcohol was added to each tube and incubated at room temperature for 10 min. The samples were centrifuged at 4°C for 15 min at 12,000 x g. The supernatant was removed, and the pellets were washed with 1 mL of 75% ethanol. Next, the samples were centrifuged at 4°C for 5 min at 12,000 x g. The supernatant was removed, and the pellets air-dried for 30 min. The pellet was then resuspended in 20 $\mu$L of RNase-free water. The samples were heated at 55°C for 15 min, chilled on ice for 2 min, and then briefly centrifuged. The RNA concentration was measured using a Nanodrop spectrophotometer. The RNA, at a concentration 1$\mu$g/$\mu$L, was electrophoresed in a 1% agarose gel to determine the quality of the sample.

cDNA Synthesis

cDNA was synthesized from extracted RNA using MultiScribe Reverse Transcriptase (Applied Biosystems, Foster City, CA). In a labeled microcentrifuge tube, 2 $\mu$g RNA, 1 $\mu$L of 100$\mu$M oligo(dT), 1 $\mu$L of 10mM dNTP were added, and then milliQ

water was added until the total volume was 13 $\mu$L. The samples were incubated at 65°C for 5 min, then placed on ice for 2 min. After briefly centrifuging the samples, 4 $\mu$L of 5 x First Strand Buffer and 2 $\mu$L 0.1 M DTT were added to each microcentrifuge tube. The samples were briefly centrifuged again, and 1 $\mu$L of MultiScribe Reverse Transcriptase was added to each tube and mixed by pipetting. The samples were incubated in a water bath at 42°C for 50 min, and the reaction was stopped by heating at 70°C for 15 min. The samples were chilled on ice for 2 min, briefly centrifuged, and then stored at -20°C.

Polymerase Chain Reaction (PCR)

Each reaction consisted of 5 $\mu$L 10x High Fidelity PCR Buffer, 1 $\mu$L 10 mM dNTP, 2 $\mu$L 50 mM $MgSO_4$, 1$\mu$L primer, 1 $\mu$L template DNA, 0.2 $\mu$L Platinum Taq High Fidelity DNA polymerase, and 40 $\mu$L nuclease-free water. A master mix was made which contained the appropriate amounts of the above reagents for the number of reactions being run with the exception of the template DNA. 49 $\mu$L of the master mix was placed into each microcentrifuge tube, and 1 $\mu$L of template DNA was added to each tube individually. The samples were briefly centrifuged and placed in the GeneAmp PCR System 9700 thermal cycler. The cycle settings were denature at 94°C for 30 s, anneal at 55°C for 30 s, and extend at 68°C for 1 min. A total of 40 cycles were run, and the samples cooled at 4°C after cycling.

Quantitative Real-Time Polymerase Chain Reaction (qRT-PCR)

All qRT-PCR reactions were performed using an ABI 7500 Fast System (Applied Biosystems, Rockville, MD). Each reaction consisted of 5 $\mu$L SYBR-green mix, 1 $\mu$L primer, 1 $\mu$L cDNA, and 3 $\mu$L nuclease-free water in a total volume of 10 $\mu$L. A master mix lacking template was made which contained the appropriate amount of the above reagents for the number of reactions being run. Each sample was run in triplicate. 9 $\mu$L of the master mix was placed into each well, and 1 $\mu$L of cDNA template was pipetted individually into each well. The 96-well plate was covered with an adhesive cover slip, and then briefly centrifuged. The 7500 Fast Real-Time PCR System was used in the Standard 7500 mode using a SYBR-green protocol.

Immunoprecipitation

Cells were counted and plated in normal growth medium. After 24 h, cells were washed with PBS and placed in serum-free medium. The conditioned medium was collected from the cells and transferred to a microcentrifuge tube. 1$\mu$g DKK3 antibody was added to each tube per 1mL of conditioned medium. The microcentrifuge tubes were rotated end-over-end at 4°C for 30 min. Next, 30$\mu$L of a 50% slurry of Protein A-Sepharose was added to each sample and rotated end-over-end for 1h at 4°C. The samples were centrifuged at 10,000 rpm for 5 min at 4°C. The supernatant was carefully decanted from each sample. 1mL of lysis buffer was added to each tube, flicked to wash, and centrifuged for 1 min. The process of removing the supernatant, washing, and centrifuging was repeated twice. After the third wash, the samples were centrifuged again without any

lysis buffer, and the remaining liquid was removed by careful pipetting. The Sepharose complexes were resuspended in 1 x SDS/PAGE buffer, heated at 95°C for 10 min, and run on a 10% SDS-polyacrylamide gel.

Cell Migration Assay

Cell migration was assessed using wound-healing (scratch) assays. Cells were counted and plated in triplicate in 12 well plates. The cells were incubated at 37°C until 100% confluent. Once totally confluent, a sterile pipette tip was used to scratch the surface of the well, which removed a layer of cells in the scratched line. Each well was washed with PBS and replaced with growth medium. After making the scratch, the width was determined by measuring three specific points under a 5 x objective using a light microscope and AxioVision software (Carl Zeiss Microimaging, Thornwood, NY). Cells were incubated at 37°C for 8 h or 24 h, at which time, the width was measured again at the same points used at 0 h.

Statistical Analysis

Data were analyzed using Microsoft Excel and Graphpad QuickCalcs software (http://www.graphpad.com/quickcalcs/). Paired T-tests were performed, and p-values were compared to an a-value of 0.05 to be considered statistically significant. Error bars on the figures represent the standard error of the mean.

## Results

### Overexpression of Vimentin in Vimentin-negative HN4 Cells

Previous research in our laboratory has shown that HN4 cells express low levels of vimentin, while HN12 cells express high levels of vimentin. Using shRNA to inhibit vimentin expression in HN12 cells, there was decreased proliferation and motility, as well as re-expression of keratins (Paccione et al., 2008). The cause of keratin re-expression is unknown, but it is possible that vimentin plays a role in this regulation directly or indirectly. Furthermore, studies have shown that Wnt signaling can upregulate vimentin expression through ß-catenin (Goto et al., 2003). Wnt-5a has been shown to increase cell motility and vimentin expression in melanoma cells. These effects are partially dependent on PKC activity (Dissanayake et al., 2007). Additionally, PKCe phosphorylates vimentin and has been shown to be required for vimentin-induced cell migration. Cells with unphosphorylatable versions of vimentin do not show increased motility (Ivaska et al., 2005). To explore the possibility of vimentin regulation of keratin, we expressed plasmids encoding wild-type vimentin, a PKCe-phosphomimetic (aspartate mutant) version of vimentin, or an unphosphorylatable (alanine mutant) version of vimentin in vimentin-negative HN4 cells. Transfection was performed using a Nucleofector device, and stable cell pools were isolated in media containing 400$\mu$g/mL G418. Vimentin overexpression was determined by western blot analysis. As shown in Fig. 4, vimentin was overexpressed

in cells containing the wild-type vimentin plasmid compared to parental HN4 cells. This overexpression was highest in clone 3, which was chosen for further experiments. Fig. 5 shows the overexpression of vimentin with the PKCe-phosphomimetic version of vimentin. The strongest overexpression was shown in clone 4, and this clone was used for subsequent studies. Overexpression of the unphosphorylatable version of vimentin is illustrated in Fig. 6. Several clones showed an increased level of vimentin compared to parental HN4 cells, but clone 5 was used for further experiments. Once these clones were identified, vimentin and keratin expression were confirmed by western blot analysis. As shown in Fig. 7, vimentin was readily detected in the HN12 cell lysates, not detectable in the HN4 cell lysates, and detectable at lower levels in cell lysates from the HN4 vimentin mutants. Additionally, keratin 14 expression was not detected in the HN12 cell lysates. However, keratin 14 was detectable in the HN4 control and vimentin mutant cell lysates. Keratin 14 expression was also confirmed by qRT-PCR, using keratin 14-specific primers. Fig. 8 shows that keratin 14 is expressed in the HN4 vimentin mutants but at a decreased level compared to HN4 control cells. Furthermore, immunofluorescence confirmed vimentin and keratin 14 expression in the HN4 vimentin mutant cells (Figs. 9 and 10, respectively). Vimentin staining was absent in HN4 control cells, and keratin 14 staining was absent in HN12 cells. These data confirm that vimentin is overexpressed in HN4 vimentin mutant cells. It also confirms that there is a difference in the expression of keratin 14 in the HN4 vimentin mutant cells compared to vector-transfected HN4 cells.

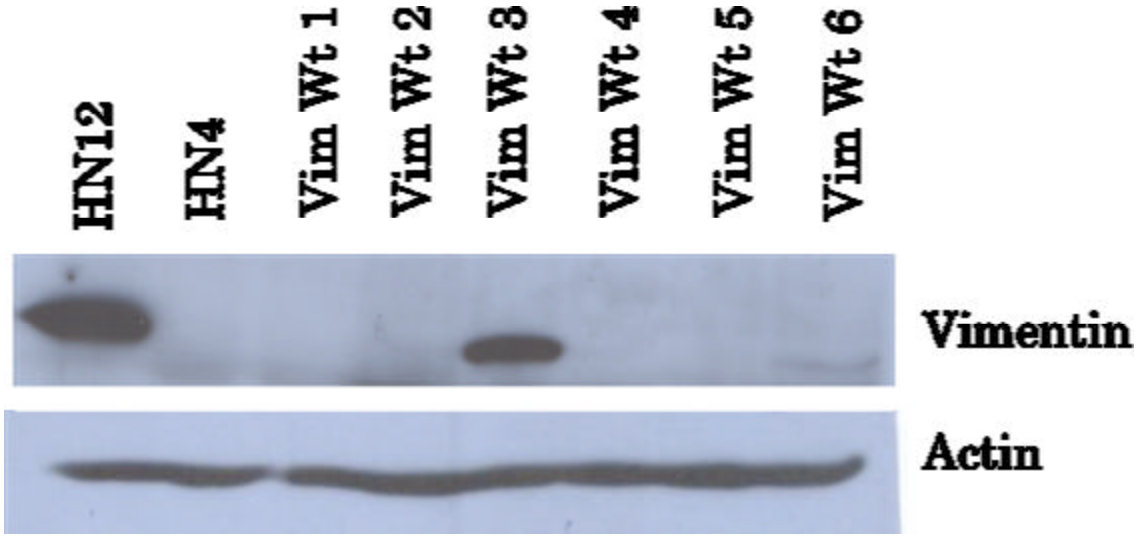


**Figure 4: Vimentin is expressed in HN4 cells transfected with the plasmid encoding wild-type vimentin.** Total cell protein extracts were prepared as described in 'Methods' and analyzed for vimentin expression by western blotting (top panel). Levels of actin were determined as a loading control (lower panel).

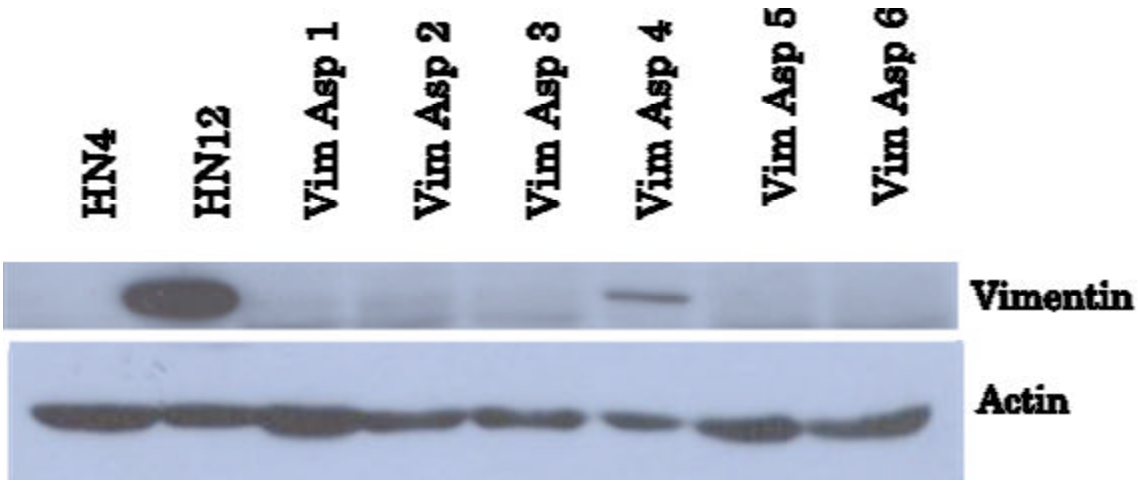


**Figure 5: Vimentin is expressed in HN4 cells transfected with the plasmid encoding a PKCe-phosphomimetic (aspartate mutant) version of vimentin.** Total cell protein extracts were prepared as described in 'Methods' and analyzed for vimentin expression by western blotting (top panel). Levels of actin were determined as a loading control (lower panel).

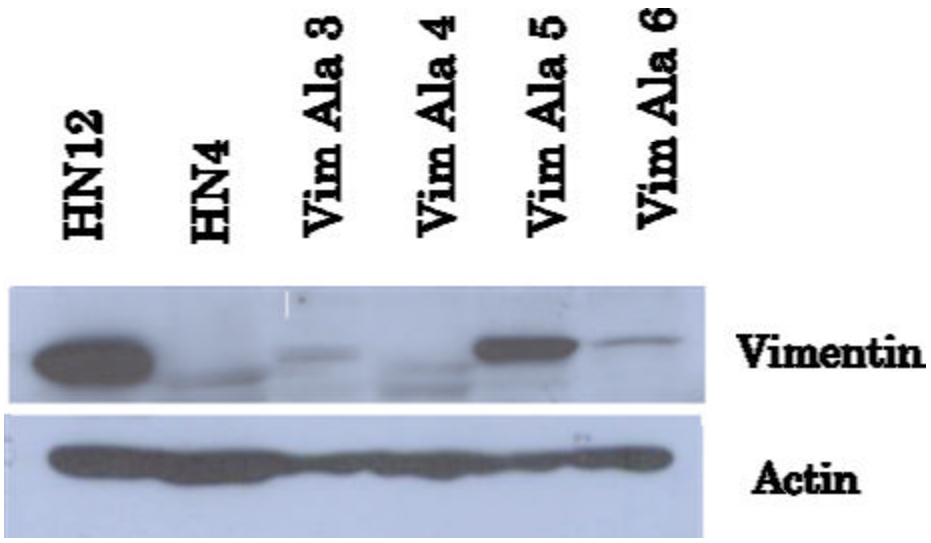


**Figure 6: Vimentin is expressed in HN4 cells transfected with the plasmid encoding an unphosphorylatable (alanine mutant) version of vimentin.** Total cell protein extracts were prepared as described in 'Methods' and analyzed for vimentin expression by western blotting (top panel). Levels of actin were determined as a loading control (lower panel).

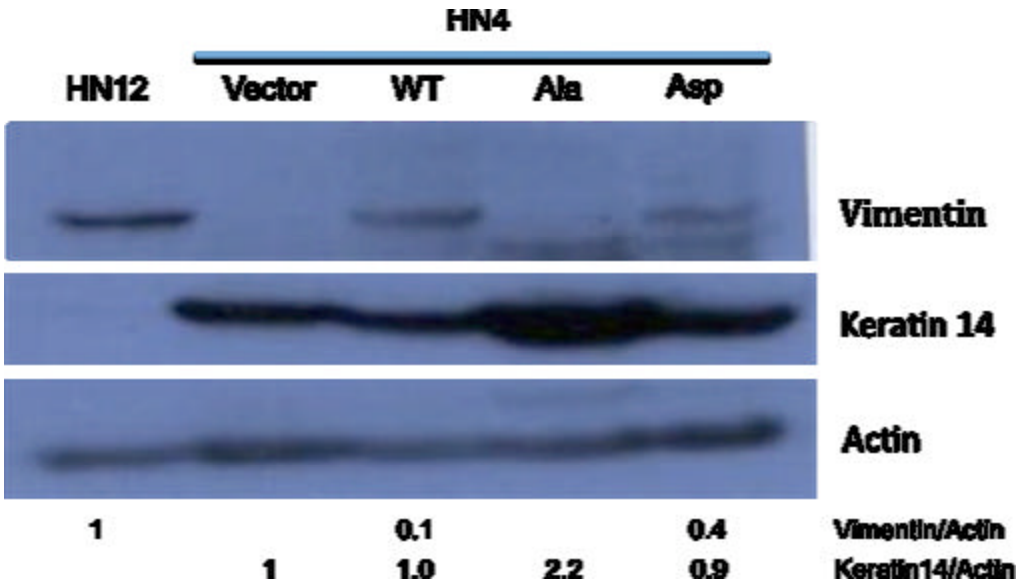


**Figure 7: Vimentin and keratin 14 expression in HN4 vimentin-transfected cells.** Total cell protein extracts were prepared as described in 'Methods' and analyzed for vimentin expression (top panel) and keratin 14 expression by western blotting (middle panel). Levels of actin were determined as a loading control (lower panel).

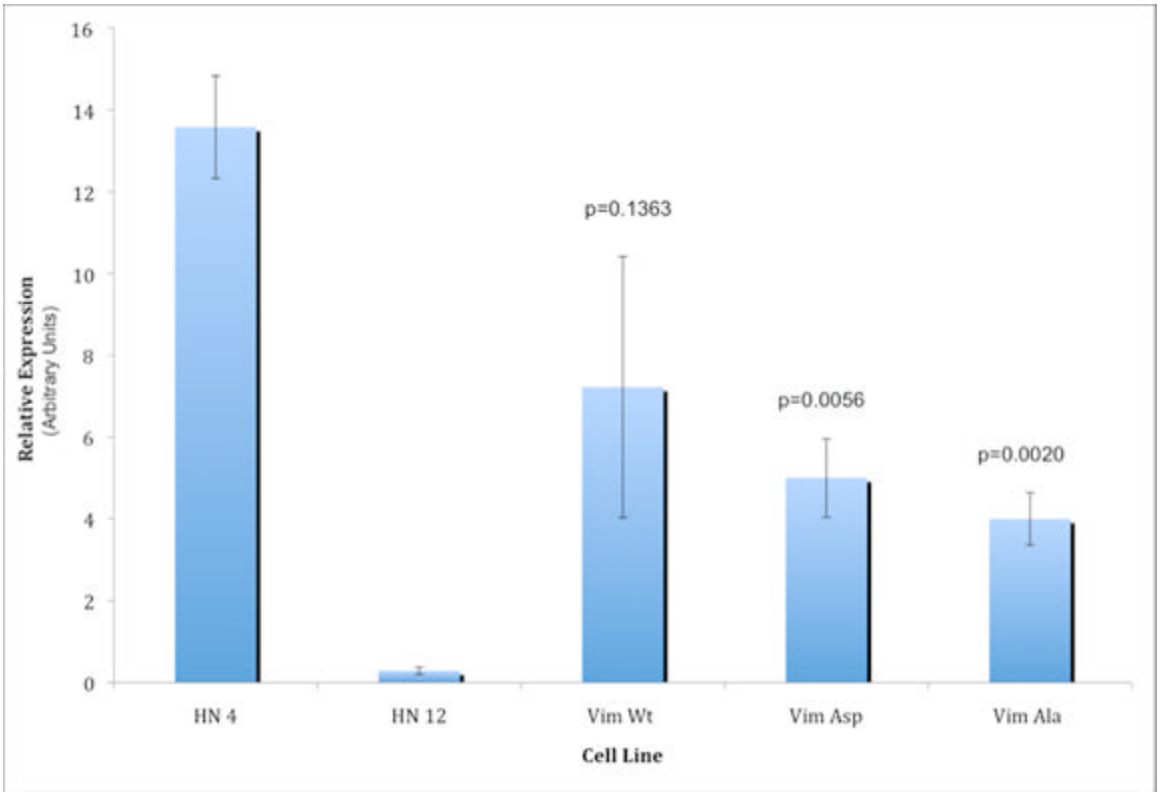


**Figure 8: Keratin 14 expression is decreased in HN4 vimentin-transfected cell lines.** Total RNA was extracted and reverse-transcribed to create cDNA, and then qRT-PCR was performed as described in 'Methods.' The relative expression ratio represents the expression of keratin 14 to the internal standard, actin.

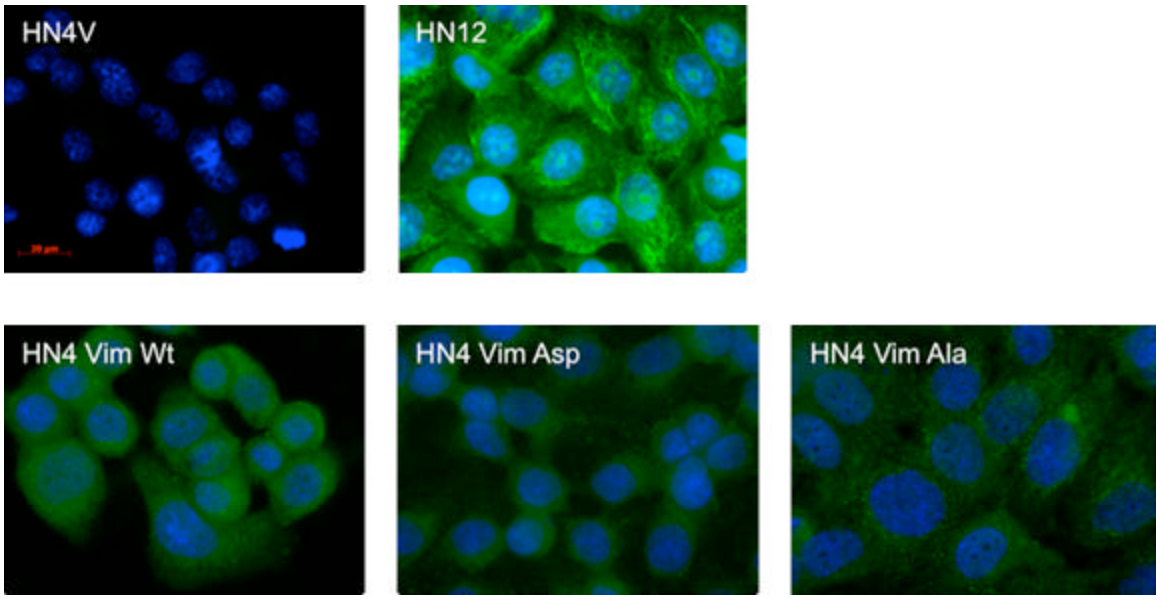


**Figure 9: Confirmation of vimentin expression in HN4 vimentin mutant cells using immunofluorescence.** Cells were cultured on glass coverslips and fixed as described in 'Methods.' Cells were incubated with anti-vimentin antibody overnight then incubated with a FITC-conjugated anti-mouse antibody for 1h and counterstained with DAPI.

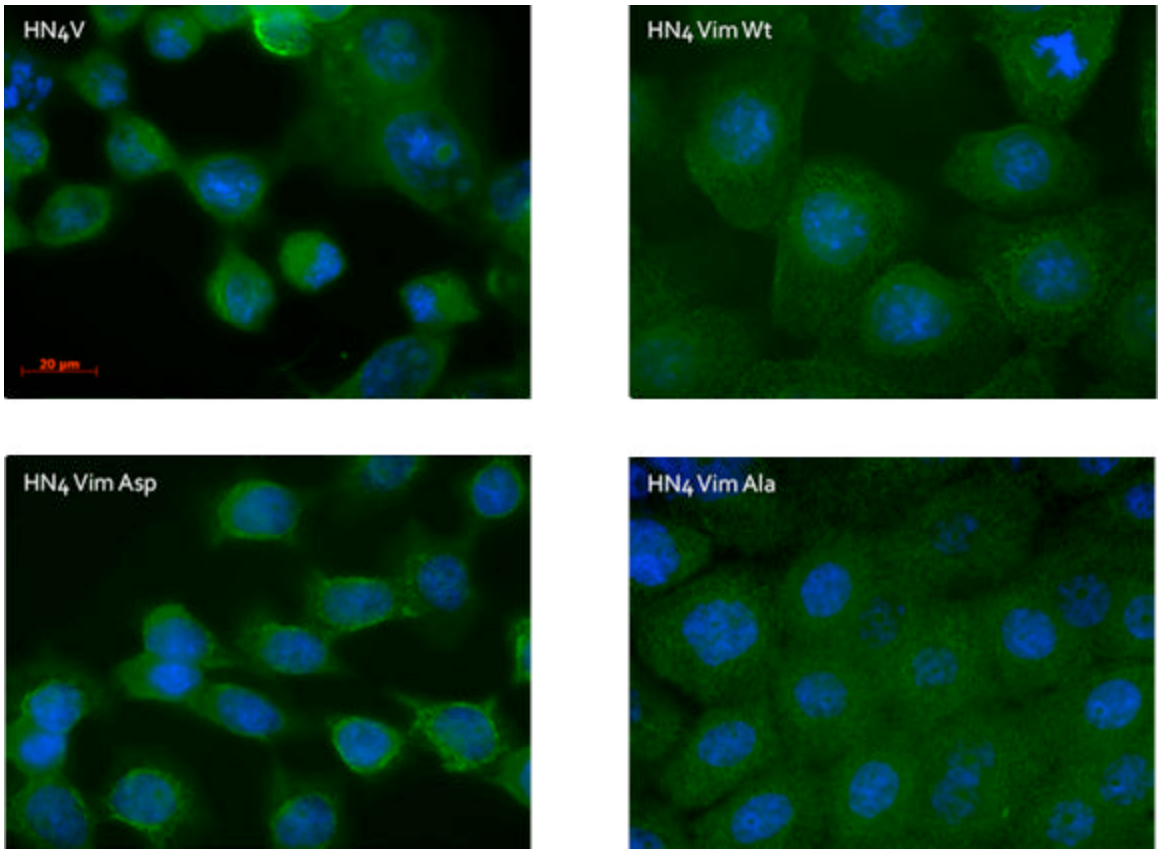


**Figure 10: Confirmation of keratin 14 expression in HN4 vimentin mutant cells using immunofluorescence.** Cells were cultured on glass coverslips and fixed as described in 'Methods.' Cells were incubated with anti-keratin 14 antibody overnight then incubated with a FITC-conjugated anti-mouse antibody for 1h and counterstained with DAPI.

Confirmation of Expression of Vimentin Mutants in 293T Cells

The pCMV Vim-Wt, Vim-Asp, and Vim-Ala plasmids were transiently transfected into 293T cells to confirm vimentin expression. qRT-PCR was performed on the cDNA template using vimentin-specific primers. Fig. 11 shows vimentin expression was higher in all three cell lines transfected with the plasmid when compared to the GFP control. The vimentin expression in the 293T cells transfected with the PKCe-phosphomimetic version of vimentin (lower panel) was much greater than the wild-type and unphosphorylatable versions of vimentin (upper panel). These data confirm that expression of these plasmids increased vimentin expression.

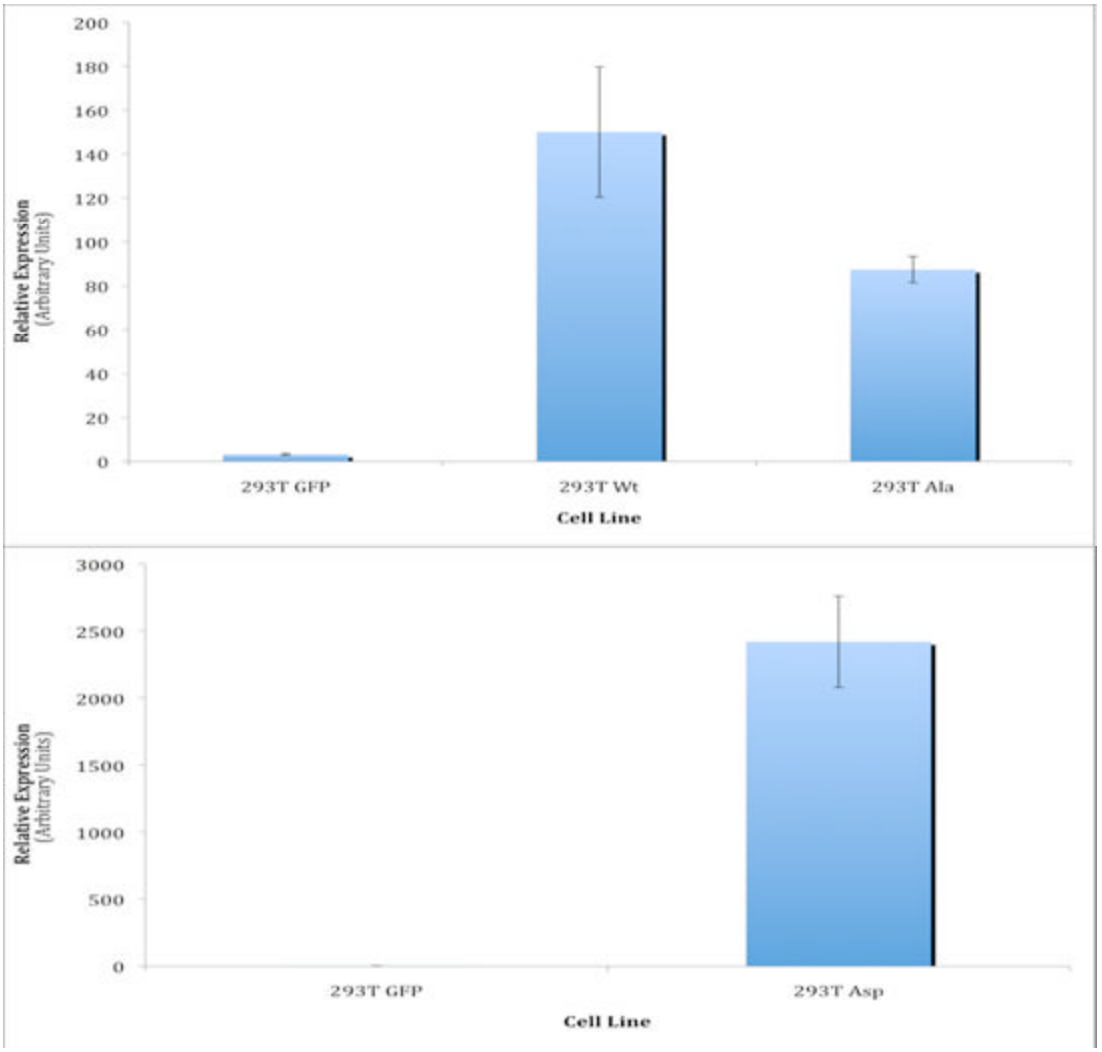


**Figure 11: Vimentin expression in transiently transfected 293T cells confirmed by qRT-PCR.** The expression ratio is a result of the vimentin expression levels compared to an internal standard, ?-tubulin. All three vimentin mutants displayed greater vimentin expression than the GFP control. However, vimentin expression in the PKCe-phosphomimetic version of vimentin (lower panel) was higher than the vimentin expression in the wild-type and unphosphorylatable version of vimentin (upper panel).

Effect of Vimentin Overexpression in HN4 Cells on Cell Growth

The expression of vimentin in HN12 cells has been suggested to cause increased proliferation, migration, and invasion when compared to HN4 cells or HN12 cells with RNAi to inhibit vimentin expression (Paccione et al., 2008). To determine the effect of vimentin overexpression in vimentin-negative HN4 cells, we performed an MTT assay on these cells to determine cell growth and viability. Cells were counted, plated in triplicate, and allowed to grow for 7 days. After 7 days, the MTT assay was performed, and the absorbance was measured by spectrophotometer. As shown in Fig. 12, the cells with the wild-type or PKCe-phosphomimetic versions of vimentin grew much faster than the cells with the unphosphorylatable version of vimentin and HN4 vector cells. Additionally, the growth of the cells with the unphosphorylatable version of vimentin was slightly slower than the HN4 vector cells. Further study of the effect on growth was carried out using a cell proliferation assay. Cells were plated in triplicate and counted over 10 days. Fig. 13 shows that cells expressing the wild-type or PKCe-phosphomimetic versions of vimentin have significantly increased proliferation compared to HN4 vector control cells. Also, proliferation of cells containing the unphosphorylatable version of vimentin is significantly decreased in comparison to HN4 vector control cells. These results suggest that vimentin phosphorylation may influence how vimentin regulates cell growth.

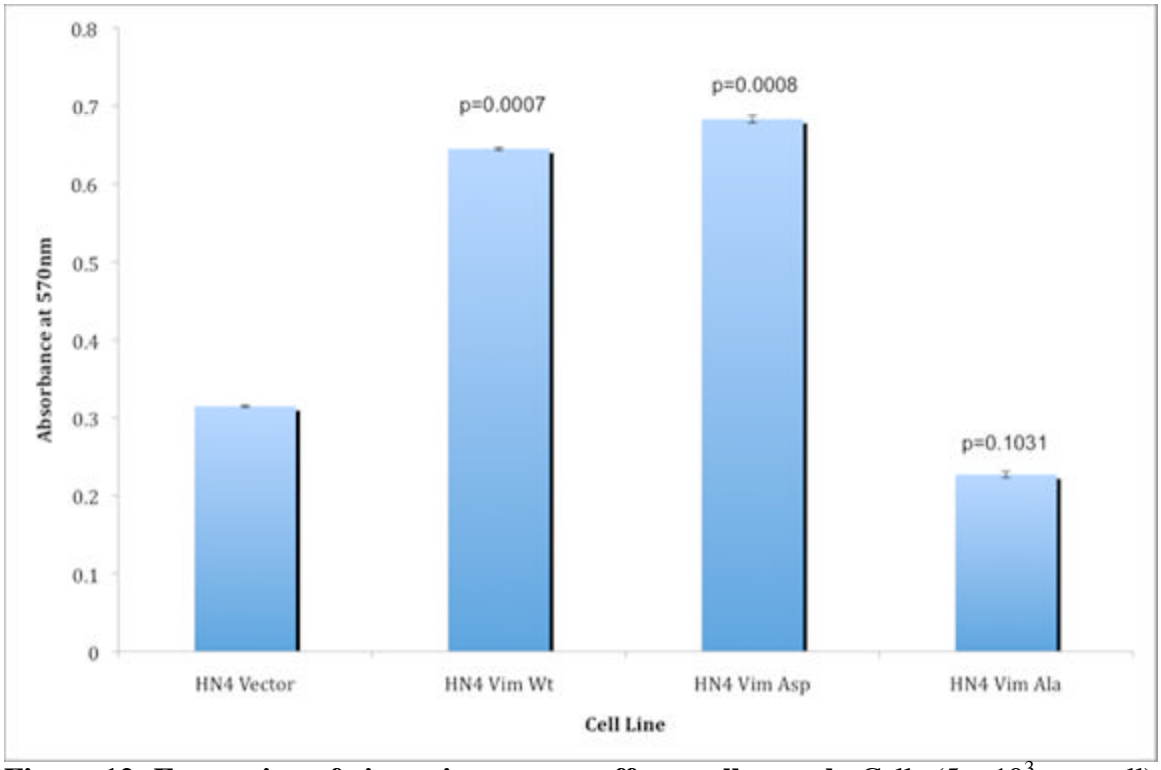


**Figure 12: Expression of vimentin mutants affects cell growth.** Cells (5 x $10^3$ per well) were plated in triplicate in 12-well plates and incubated as described in 'Methods.' After 7 days, the MTT assay was performed.

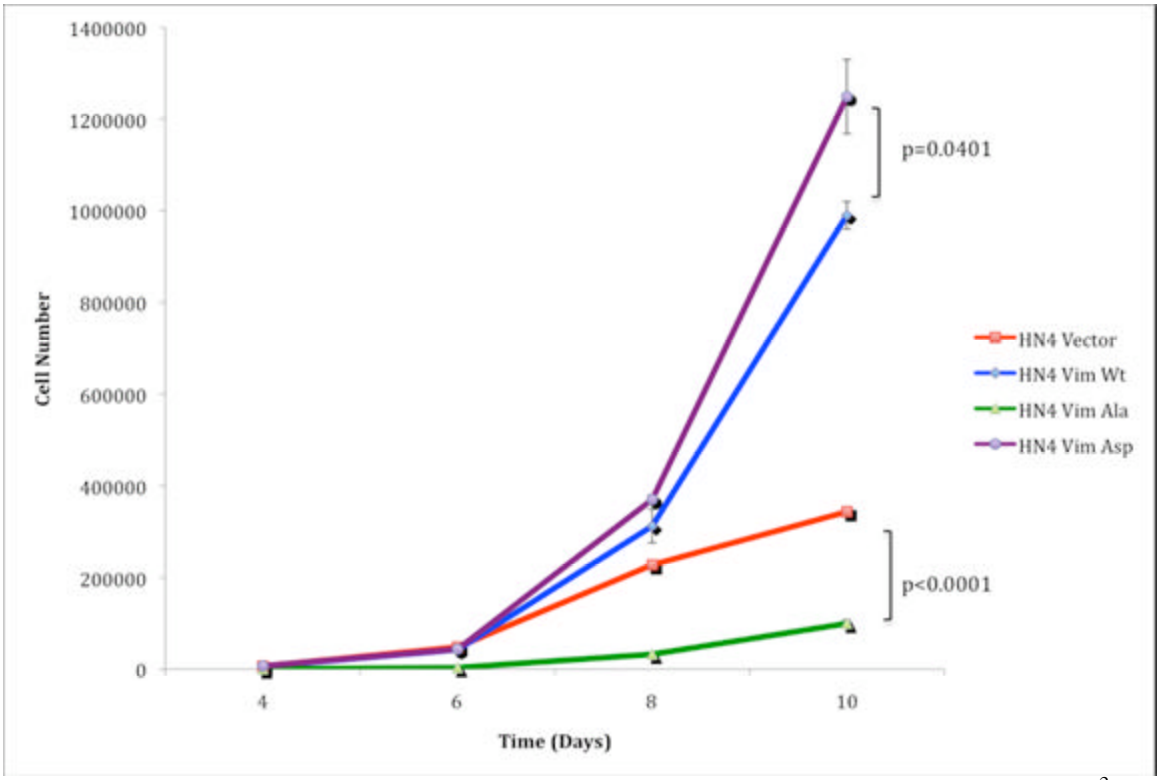


**Figure 13: Expression of vimentin mutants affects cell proliferation.** Cells (5 x $10^3$ per well) were plated in triplicate in 6-well plates and incubated as described in 'Methods.' Cell counting began 4 days after cells were plated, and they were counted every other day until day 10.

Effect of Vimentin Overexpression in HN4 Cells on Cell Motility

After determining the effect of vimentin overexpression on proliferation of HN4 cells, we were interested to find out whether this overexpression also affected cell motility. To determine the effect of vimentin overexpression on cell motility, we performed a wound-healing (scratch) assay. Cells were counted, plated in triplicate, and allowed to grow until 100% confluent. The wells were scratched with a sterile pipette tip, and the width of the scratch was measured using a light microscope. Once the scratch was measured at 0h, the cells were re-placed in the incubator, and the scratch was measured again 8h or 24h later. As shown in Fig. 14, the cells with wild-type or PKCe-phosphomimetic versions of vimentin migrated at a faster rate than the HN4 vector cells. Additionally, the cells with the unphosphorylatable version of vimentin migrated at a rate similar to the HN4 vector cells.

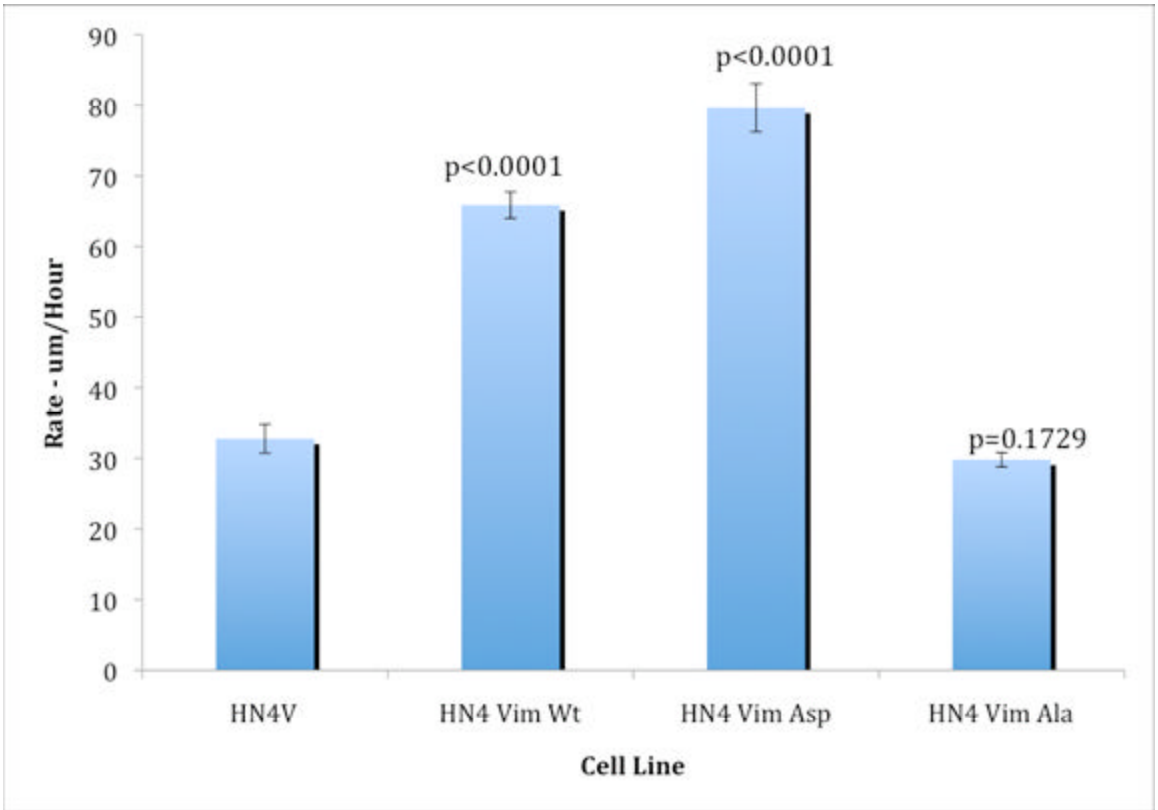


**Figure 14: Expression of Vimentin Mutants Affects Cell Motility.** Cells were plated in triplicate in 12-well plates and incubated under standard conditions. Wells were scratched, and the width was measured as described in 'Methods.'

Effect of Vimentin Overexpression in HN4 Cells on the Presence of ß-catenin

Research shows that ß-catenin can stimulate vimentin expression (Gilles et al., 2003). Since we have overexpressed vimentin in these HN4 cells, we were interested in whether ß-catenin showed altered expression. Immunofluorescence confirmed the expression of ß-catenin in the HN4 vimentin mutants, as seen in Fig. 15. All of the cell lines express ß-catenin, and there appears to be little difference in the staining between the various mutants either in terms of intensity or localization.

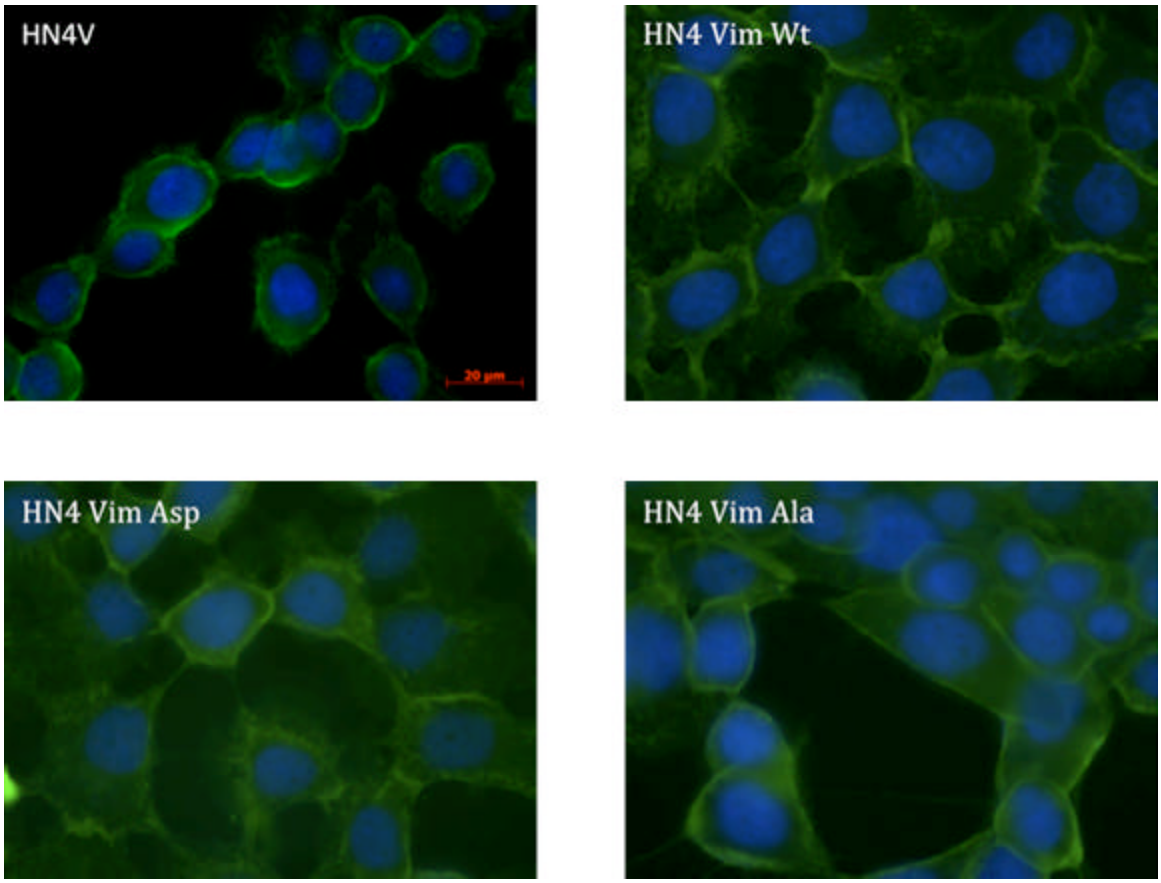


**Figure 15: ß-catenin expression in HN4 vimentin-transfected cells.** Cells were cultured on glass coverslips and fixed as described in 'Methods.' Cells were incubated with anti-ß-catenin antibody overnight, and then incubated with a FITC-conjugated anti-goat antibody for 1h and counterstained with DAPI.

Effect of Vimentin Overexpression in HN4 Cells on the Presence of E-cadherin

E-cadherin is a major molecule in the adherens junction, and it plays are large role in EMT due to its interaction with ß-catenin (Voulgari & Pintzas, 2009). In tumorigenesis, E-cadherin is commonly inactivated or silenced by various mechanisms. We used immunofluorescence to determine whether the presence of vimentin in HN4 cells affects or alters the expression of E-cadherin. Our results show distribution of E-cadherin is altered in cells expressing wild-type or mutant forms of vimentin. As seen in Fig. 16, cells encoding the wild-type version of vimentin show E-cadherin staining resembling the HN4V control cells. However, there are distinct changes in the other two vimentin expressing mutants. In cells encoding the PKCe-phosphomimetic version of vimentin, the E-cadherin is present in packets throughout the cytoplasm. Cells encoding the unphosphorylatable version of vimentin show a variety of different E-cadherin patterns, and the entire sample consisted of the variations shown in Fig. 16. Clearly, the expression of E-cadherin is altered in cells encoding the unphosphorylatable version of vimentin.

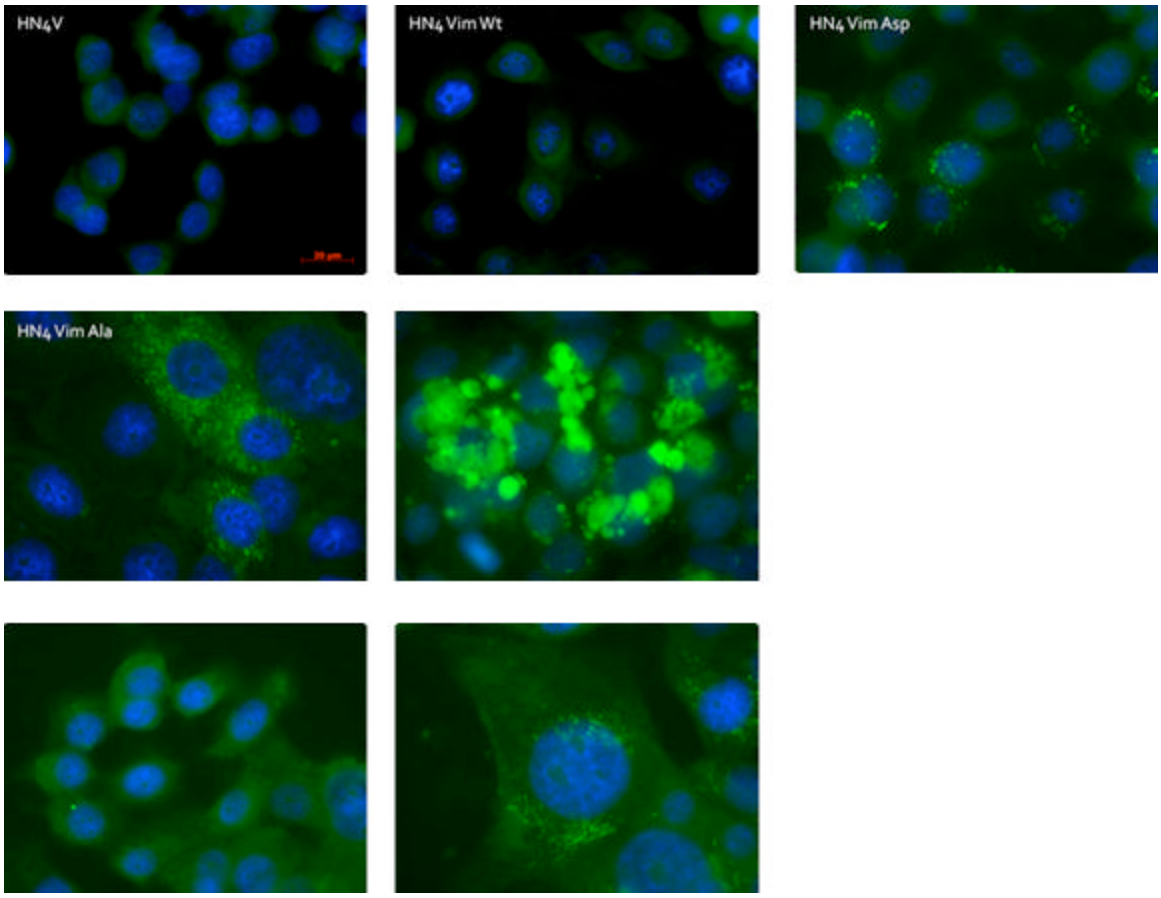


**Figure 16: E-cadherin expression in HN4 vimentin-transfected cells.** Cells were cultured on glass coverslips and fixed as described in 'Methods.' Cells were incubated with anti-E-cadherin antibody overnight, and then incubated with a FITC-conjugated anti-rat antibody for 1h and counterstained with DAPI.

NF-?B Inhibitor Effects Vimentin-Positive HN12 Cells

Previous research in our lab showed an increase in K13, K14, and K15 expression in vimentin knock-down cells. Additionally, studies have shown that NF-?B transcription factors may be involved in keratin repression (Blumenberg, 2006). Also, NF-?B is commonly involved in tumor progression. To examine the effect of NF-?B on vimentin and keratin expression, we used an NF-?B inhibitor on vimentin-positive HN12 cells. Initially, we performed an MTT assay to determine the appropriate concentration of NF-?B inhibitor to use without being toxic to the cells. Cells were counted, plated in triplicate, and allowed to grow for 7 days. After 7 days, the MTT assay was performed, and the absorbance was measured by spectrophotometer. Fig. 17 shows the results of different NF-?B inhibitor concentrations on HN12 cells. The presence of the NF-?B inhibitor resulted in decreased HN12 cell growth. This decrease in cell growth is greater with an increasing concentration of the NF-?B inhibitor. In initial studies, we used 200nM. First, we performed a qRT-PCR on the cDNA template using vimentin-specific primers. Fig. 18 shows vimentin expression was decreased in the vimentin-positive HN12 cells after being treated with 200nM NF-?B inhibitor. After we observed a decrease in vimentin expression, we determined the effect of the NF-?B inhibitor on cell proliferation. Cells were plated in triplicate and counted over 8 days. Fig. 19 shows that the presence of 200nM NF-?B inhibitor also resulted in decreased proliferation of vimentin-positive HN12 cells.

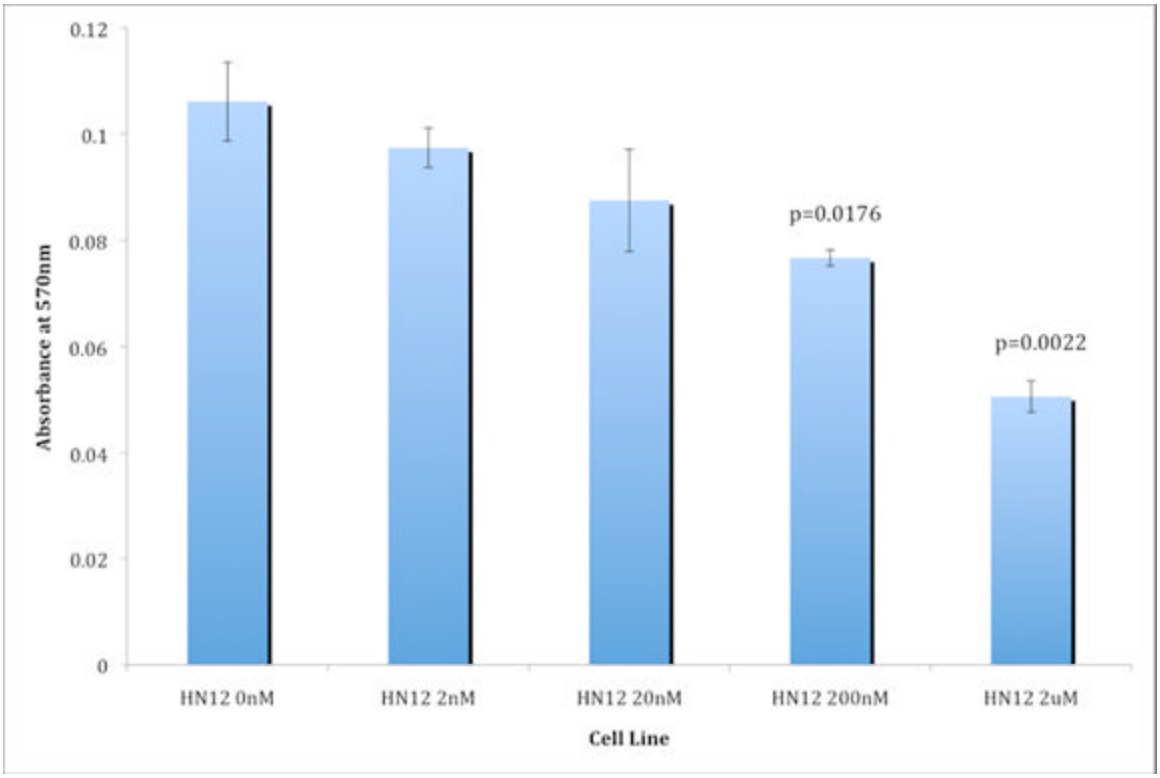


**Figure 17: Dose-response of HN12 cells with NF-?B inhibitor.** Cells (5 x $10^3$ per well) were plated in triplicate in 12-well plates and incubated as described in 'Methods.' After 7 days, the MTT assay was performed.

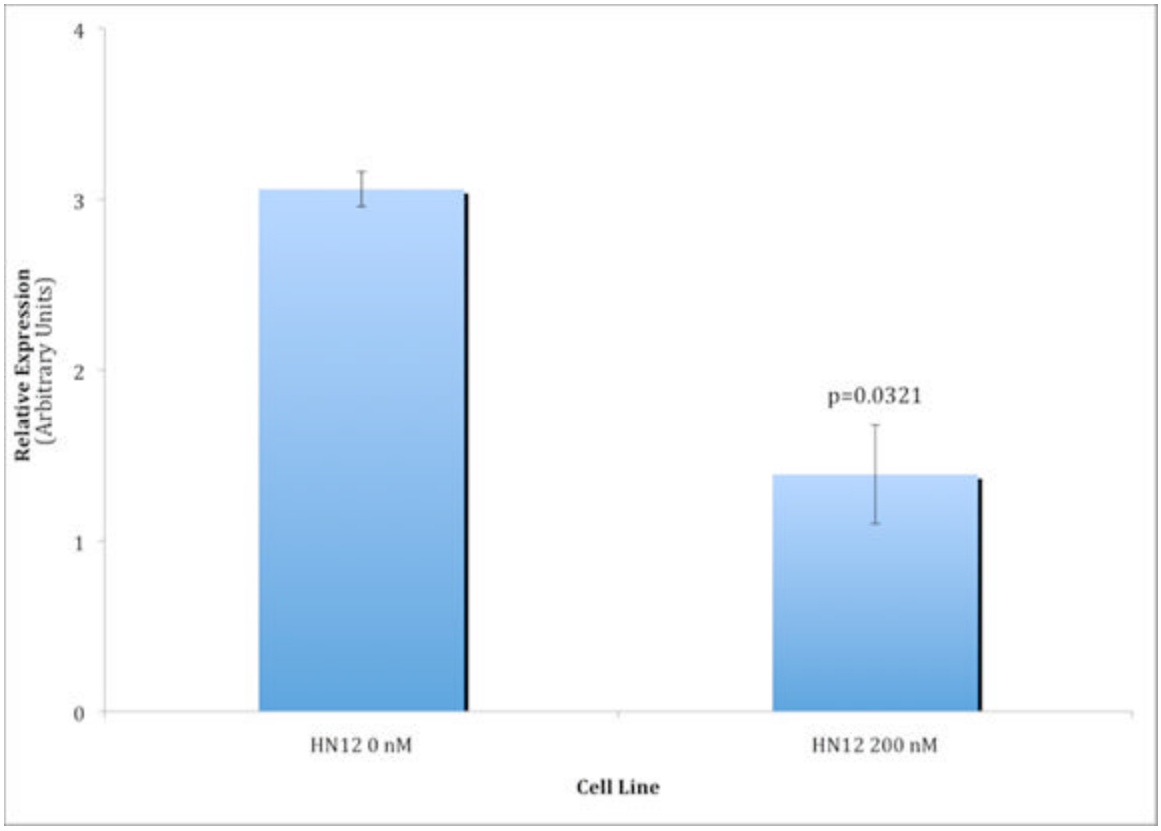


**Figure 18: NF-?B inhibition leads to reduced vimentin expression in HN12 cells.** Total RNA was extracted and reverse-transcribed to create cDNA, and then qRT-PCR was performed as described in 'Methods.' The relative expression ratio represents expression of vimentin to the internal standard actin.

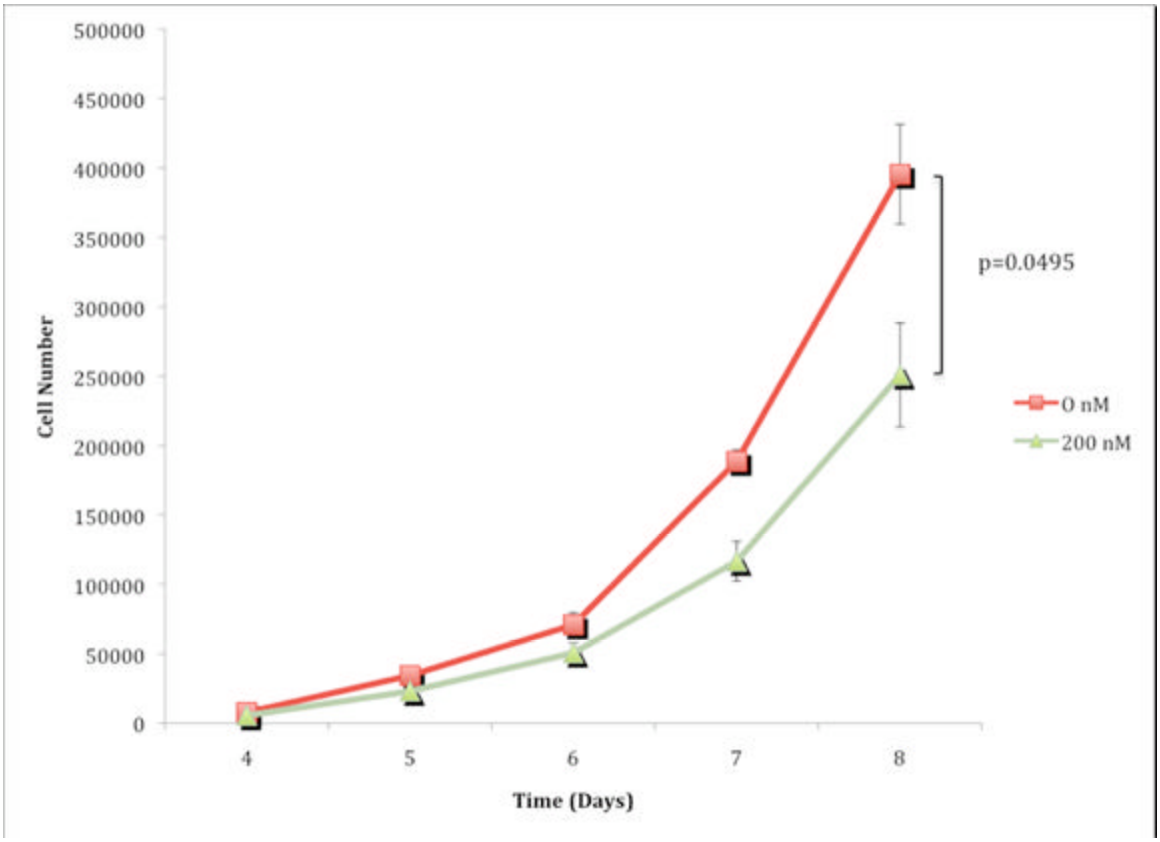


**Figure 19: NF-?B inhibition leads to reduced proliferation of HN12 cells.** Cells (5 x $10^3$ per well) were plated in triplicate in 6-well plates and incubated as described in 'Methods.' Cell counting began 4 days after cells were plated, and they were counted everyday until day 8.

5-Aza-dC Affects Vimentin-Positive HN12 Cells

Previous research in our lab suggested that the promoter of DKK3, a Wnt antagonist, is methylated in advanced HNSCC cells. This methylation represses DKK3 expression in these cells. HN12 cells grown in the presence of 5-Aza-dC removes this repression and transcriptional targets of ß-catenin are decreased. ß-catenin has also been shown to enhance vimentin expression. Therefore, it is possible that repressing DKK3 could enhance Wnt signaling and lead to increased vimentin expression, which might additionally cause decreased keratin expression. To explore the effect of 5-Aza-dC on cell growth in vimentin-positive HN12, we performed an MTT assay. Cells were counted, plated in triplicate, and allowed to grow for 7 days. After 7 days, the MTT assay was performed, and the absorbance was measured by a spectrophotometer the next day. Fig. 20 shows the result of the MTT assay. HN12 cells grown in the presence of 5-Aza-dC resulted in decreased cell growth. After seeing a decrease in cell growth by the MTT assay, we performed a cell proliferation assay on HN12 cells grown in the presence of 5-Aza-dC. In Fig. 21, the effect of 5-Aza-dC on HN12 cell proliferation is shown. When grown in the presence of 5-Aza-dC, HN12 cells have decreased proliferation.

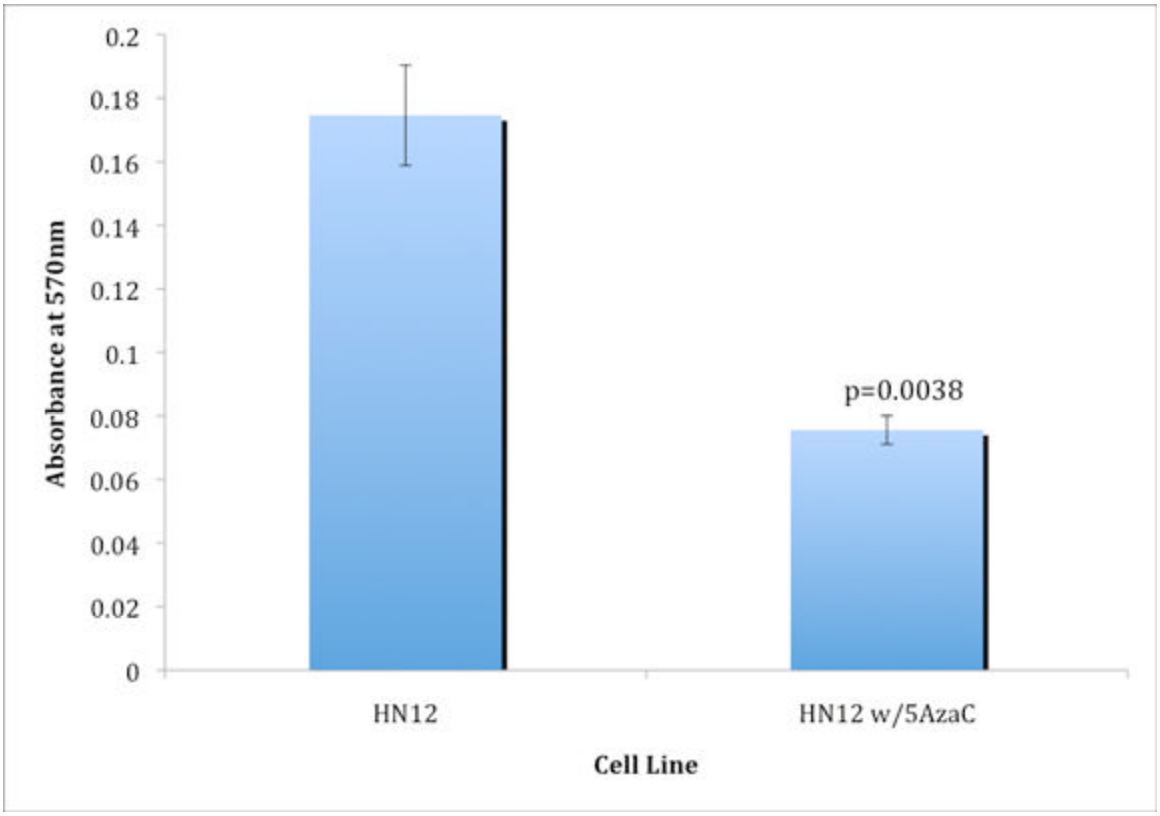


**Figure 20: 5-Aza-dC leads to reduced cell growth in HN12 cells.** Cells (5 x $10^3$ per well) were plated in triplicate in 12-well plates and incubated as described in 'Methods.' After 7 days, the MTT assay was performed.

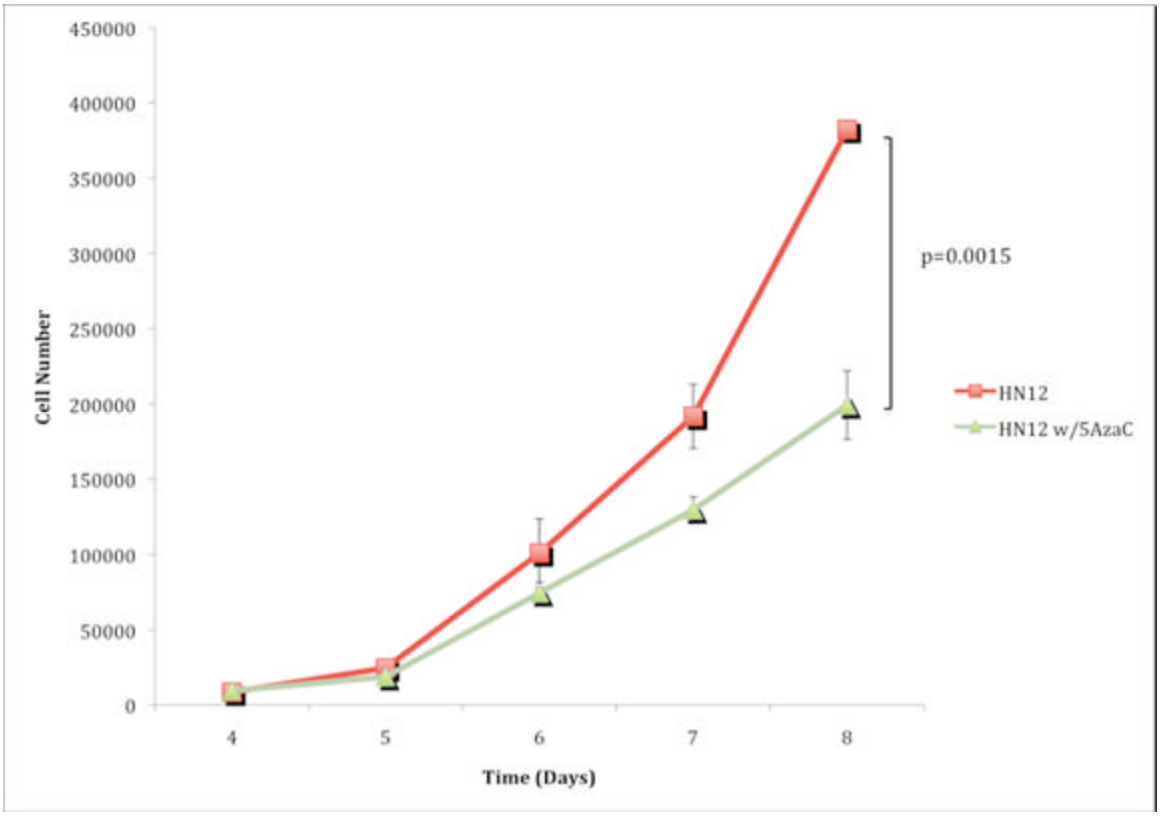


**Figure 21: 5-Aza-dC leads to reduced proliferation of HN12 cells.** Cells (5 x $10^3$ per well) were plated in triplicate in 6-well plates and incubated as described in 'Methods.' Cell counting began 4 days after cells were plated, and they were counted everyday until day 8.

Combined Effect of NF-?B Inhibitor and 5-Aza-dC on Vimentin-Positive HN12 Cells

In addition to NF-?B repressing keratin expression and methylation of DKK3 allowing Wnt signaling in HN12 cells, there is also a possibility that Wnt signaling could activate NF-?B or that these pathways might act in concert. After observing the individual effects of the NF-?B inhibitor and 5-Aza-dC on HN12 cells, we grew the cells under both conditions to see if there is a combined effect. For these experiments, we used 2$\mu$M NF-?B inhibitor. As shown in Fig. 17, this concentration provided a greater decrease in cell growth than 200 nM, but did not appear toxic to the cells. Initially, we performed a MTT assay, and Fig. 22 shows the effect of the NF-?B inhibitor, 5-Aza-dC, and the combined effect of both on HN12 cells. The growth of HN12 cells was decreased in all three conditions. However, the greatest decrease in growth was seen with the NF-?B inhibitor and the combination of the NF-?B inhibitor and 5-Aza-dC. After seeing a significant decrease at day 7, we decided to perform an MTT assay on days 5, 6, and 7 to determine if it was a gradual change. Fig. 23 shows the difference between the results on each of these three days. The greatest increase in growth appears between days 6 and 7. To explore this further, we performed a cell proliferation assay. Cells were plated in triplicate and counted over 8 days. Fig. 24 shows the results of the cell proliferation assay. Clearly, HN12 cells proliferate at a slower rate when grown in the presence of the NF-?B inhibitor or 5-Aza-dC. A greater decrease was seen again with either 2$\mu$M NF-?B inhibitor or the combination of the NF-?B inhibitor and 5-Aza-dC. Additionally, we decided to investigate vimentin expression in HN12 cells treated with these conditions using western blotting and immunofluorescence. Fig. 25 shows that vimentin was expressed in the cells treated with

the NF-?B inhibitor, 5-Aza-dC, or a combination of the two. However, vimentin expression was decreased in all of the treated cell lines, and the largest decrease was seen in the cells treated with 5-Aza-dC. The results of our immunostaining experiment are shown in Fig. 26. Again, vimentin expression is present in the cell lines treated with NF-?B inhibitor or 5-Aza-dC, but the expression is much weaker in the treated cells than the control HN12 cells.

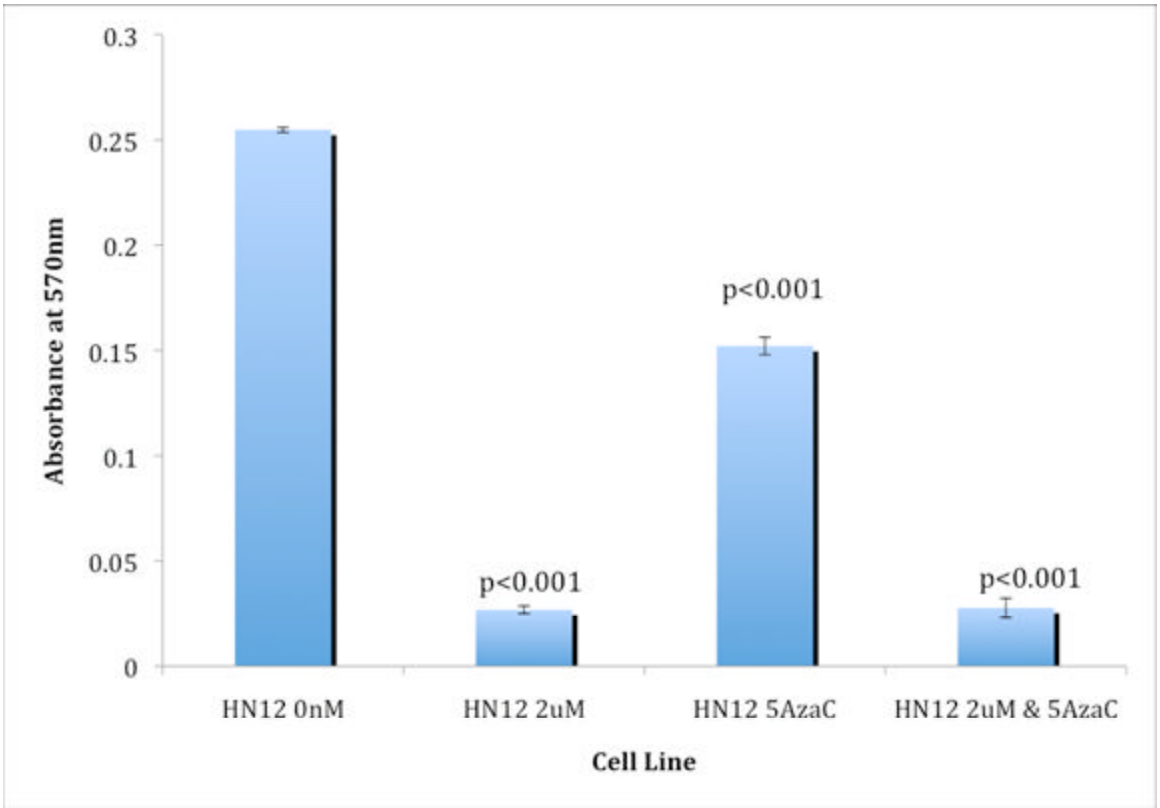


**Figure 22: NF-?B inhibitor and 5-Aza-dC reduce HN12 cell growth.** Cells (5 x $10^3$ per well) were plated in triplicate in 12-well plates and incubated as described in 'Methods.' After 7 days, the MTT assay was performed.

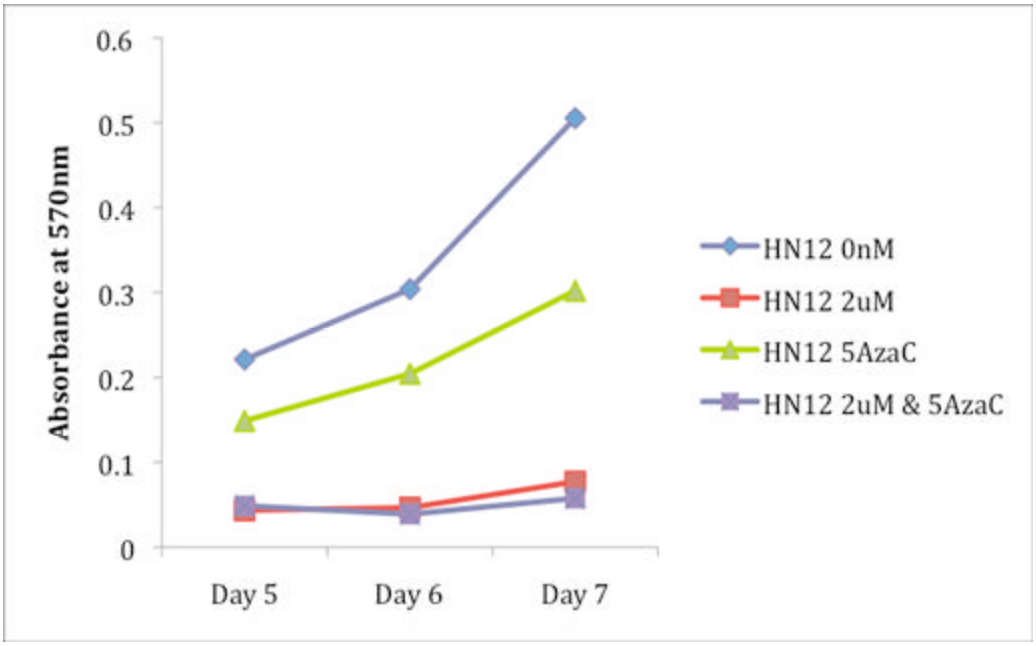


**Figure 23: Growth change as a result of NF-?B inhibitor or 5-Aza-dC is gradual.** Cells (5 x $10^3$ per well) were plated in triplicate in 12-well plates and incubated as described in 'Methods.' Three 12-well plates were plated for each set of conditions. On day 5, 6, and 7, the MTT assay was performed.

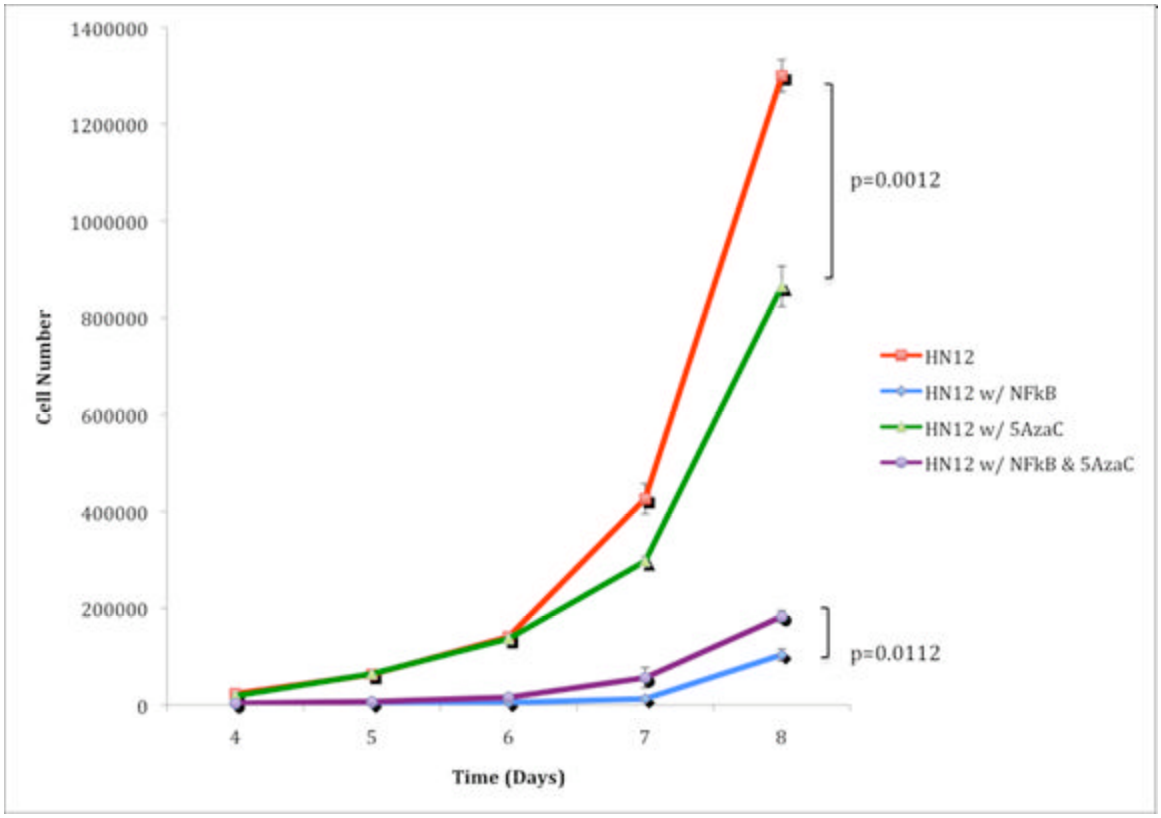


**Figure 24: NF-?B inhibitor and 5-Aza-dC reduce HN12 cell proliferation.** Cells (5 x $10^3$ per well) were plated in triplicate in 6-well plates and incubated as described in 'Methods.' Cell counting began 4 days after cells were plated, and they were counted daily until day 8.

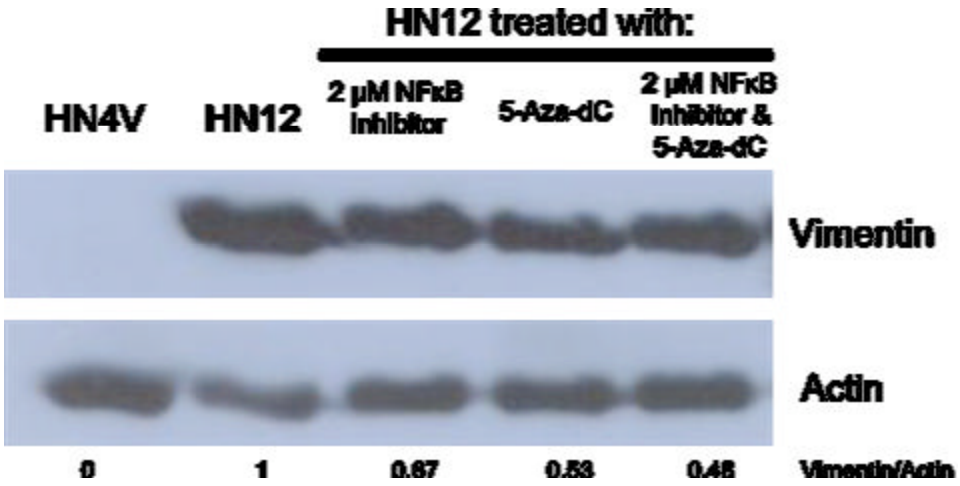


**Figure 25: Vimentin expression is decreased in HN12 cells treated with NF-?B inhibitor or 5-Aza-dC.** Total protein extracts were prepared as described in 'Methods' and analyzed for vimentin expression (top panel). Levels of actin were determined as a loading control (lower panel).

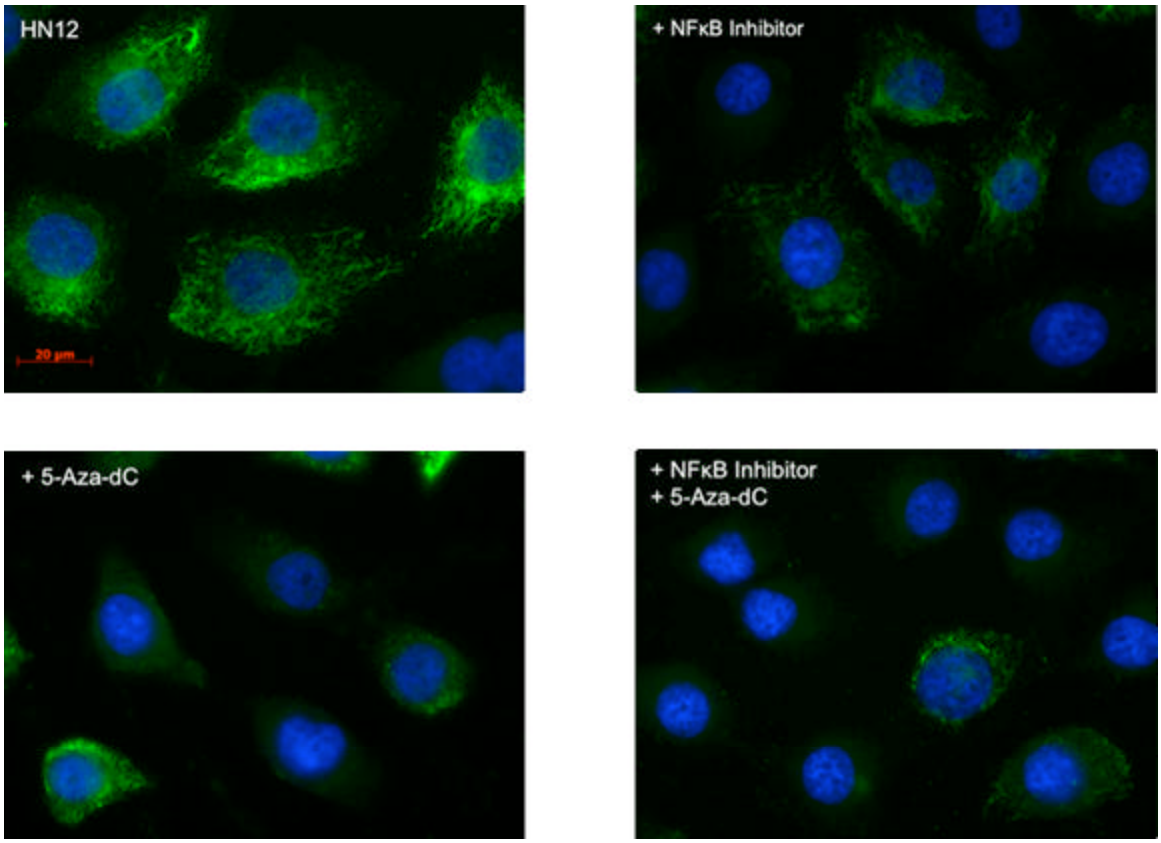


**Figure 26: Vimentin expression in HN12 cells treated with NF-?B inhibitor or 5-Aza-dC using immunofluorescence.** Cells were cultured on glass coverslips and fixed as described in 'Methods.' Cells were incubated with anti-vimentin antibody overnight, and then incubated with a FITC-conjugated anti-mouse antibody for 1h and counterstained with DAPI.

Effects of DKK3 shRNA Expression in Vimentin-negative HN4 Cells

Research in our laboratory suggests that DKK3, a Wnt antagonist, is repressed by methylation in HN12 cells. To confirm the difference of DKK3 expression in vimentin-negative HN4 cells and vimentin-positive HN12 cells, a qRT-PCR analysis was performed using DKK3-specific primers. Fig. 27 confirms there is a difference in DKK3 expression between these two cell lines, and the amount of DKK3 expressed in HN12 cells is significantly decreased compared to HN4 cells. HN4 cells that express DKK3 shRNA were previously generated in our laboratory, and we performed a qRT-PCR with DKK3-specific primers to confirm the quantity of the DKK3 inhibition. Based on the results in Fig. 28, the shDKK3 clones 1 and 4 were used for further study. After confirming the inhibition of DKK3 in these clones by qPCR, a western blot analysis was performed. As seen in Fig. 29, cell lysates from the HN4 cells had the largest amount of DKK3 expression. A decrease in DKK3 expression was seen in the HN12 cell lysates, but a much clearer decrease was shown by the HN4 shDKK3 #1 cell lysates. This western blot also illustrated that HN4 shDKK3 #4 was not a substantial DKK3 knockdown. We also detected vimentin expression in the HN4 shDKK3 #1 cell lysates. Vimentin expression was seen in the HN12 cells as well. Additionally, conditioned media from HN4 and HN4 shDKK3 cells were immunoprecipitated with a DKK3 antibody to determine DKK3 secretion from these cells. HN4, HN4 shDKK3 #1, and HN4 shDKK3 #4 cells were counted and plated in normal growth medium. After 24 h, cells were washed with PBS and placed in serum-free medium. The conditioned medium was collected from the cells, and immunoprecipitation was performed using a DKK3 antibody. Fig. 30 shows the expression of DKK3 from these

three immunoprecipitation reactions. All three samples from the immunoprecipitation reactions showed expression of DKK3, although the expression in the HN4 shDKK3 cells was slightly decreased compared to the amount of DKK3 secreted by the HN4 control cells.

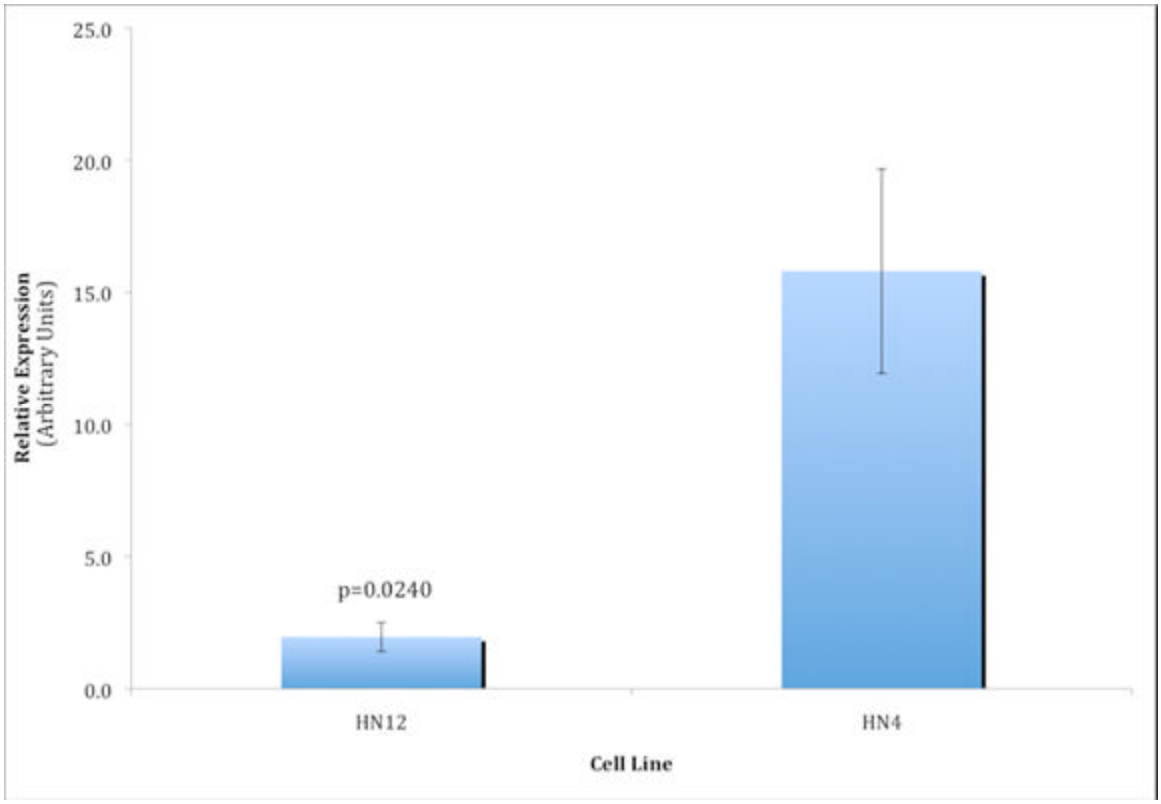


**Figure 27: Expression of DKK3 in HN12 and HN4 cells.** Total RNA was extracted and reverse-transcribed to create cDNA, and then qRT-PCR was performed as described in 'Methods.' The relative expression ratio represents the expression of DKK3 to the internal standard, actin.

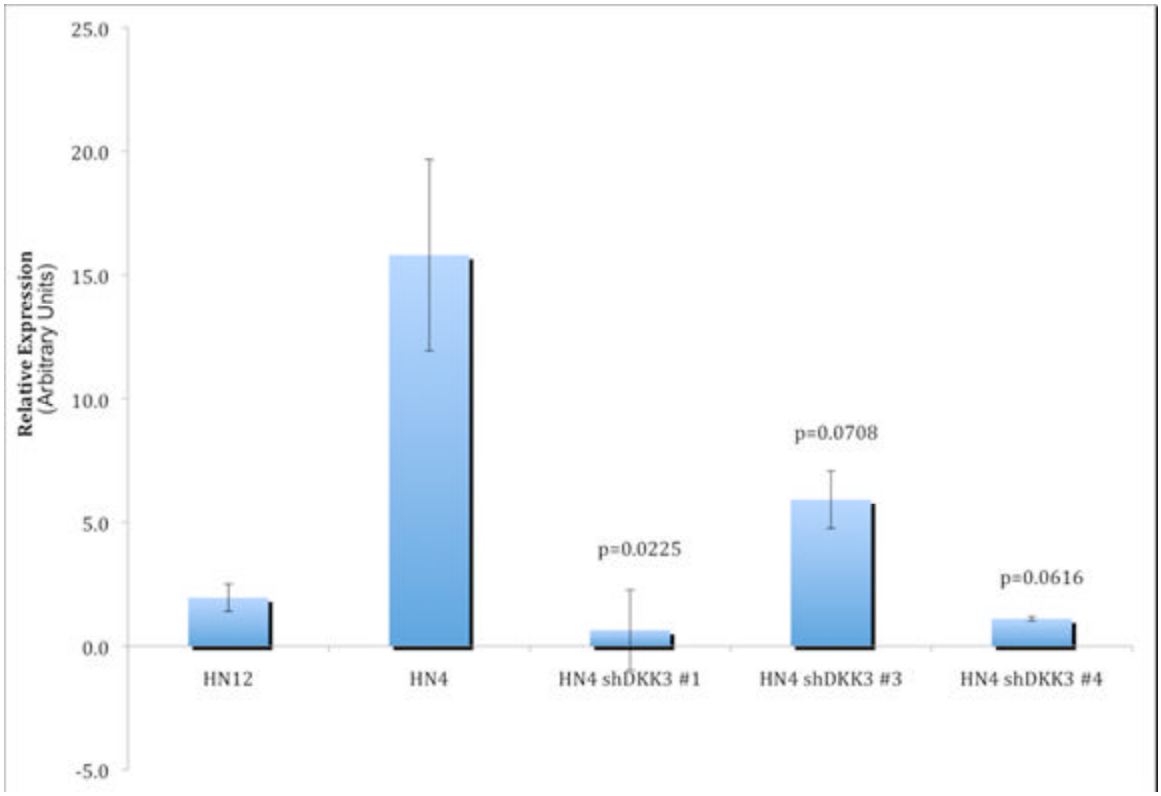


**Figure 28: shRNA-mediated inhibition of DKK3.** Total RNA was extracted and reverse-transcribed to create cDNA, and then qRT-PCR was performed as described in 'Methods.' The relative expression ratio represents the expression of DKK3 to the internal standard, actin.

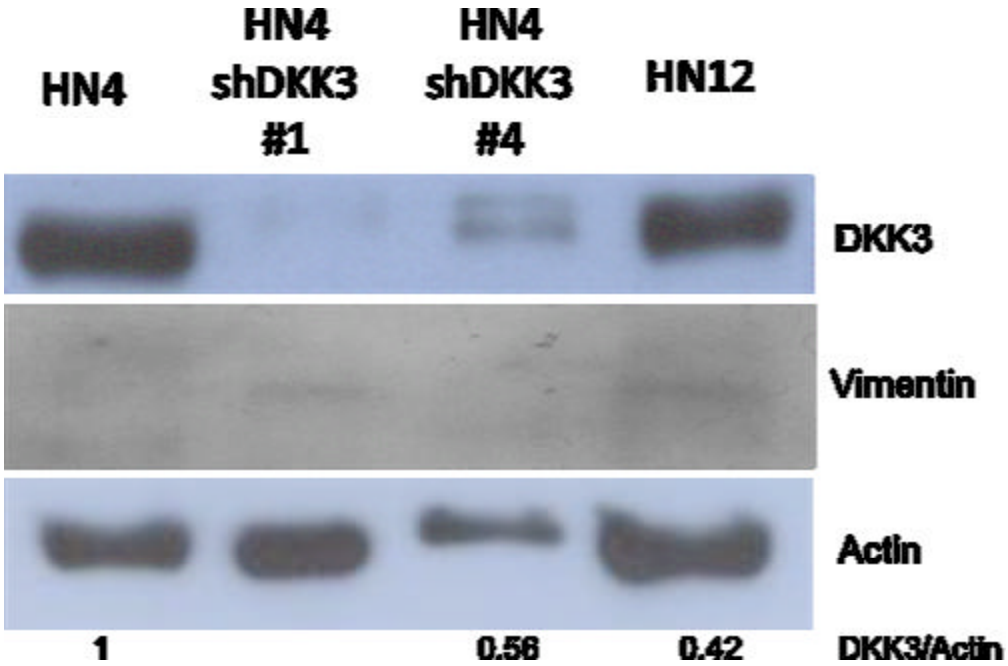


**Figure 29: DKK3 and vimentin expression in HN4 cells expressing DKK3 shRNA.**

Total cell protein extracts were prepared as described in 'Methods' and analyzed for DKK3 expression (top panel) or vimentin (middle panel). Levels of actin were determined as a loading control (lower panel).

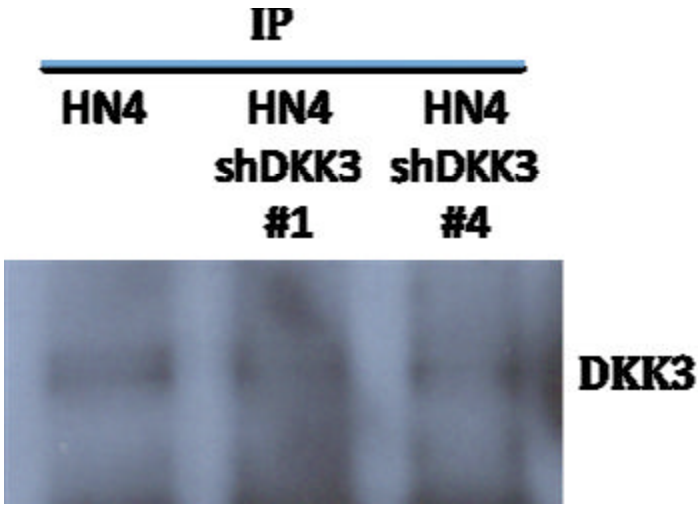


**Figure 30: DKK3 is secreted by HNSCC cells.** Cells were counted and plated in normal growth medium. After 24 h, cells were washed with PBS and placed in serum-free medium. The conditioned medium was collected from the cells, and the immunoprecipitation reaction was performed as described in 'Methods' using the DKK3 antibody.

# Discussion

## Aims of Current Study

The aims of this study were to determine keratin gene expression and biological response in cells that express wild-type and PKC phosphorylation site mutants of vimentin and to determine the role of Wnt signaling in vimentin expression during EMT.

## Overexpression of Vimentin in Vimentin-negative HN4 Cells

EMT is the process that is responsible for allowing epithelial tumors to metastasize to other tissues (Stadler et al., 2008). Undergoing EMT usually results in decreased cell anchorage and increased cell motility. Vimentin expression is associated with EMT and increased metastatic potential (Ghosh et al., 2002). EMT is also characterized by a decrease in epithelial cell markers, such as E-cadherin (Lester et al., 2007). Previous research in our lab showed that when vimentin expression is inhibited in HN12 cells by shRNA, the cells exhibited decreased proliferation and motility, as well as re-expression of keratins (Paccione et al., 2008).

To determine the effect on keratin gene expression in response to vimentin overexpression, plasmids encoding wild-type vimentin, a PKCe-phosphomimetic (aspartate mutant) version of vimentin, or an unphosphorylatable (alanine mutant) version of vimentin were expressed in vimentin-negative HN4 cells. Vimentin overexpression was

confirmed by western blot analysis, and the clone with the strongest overexpression was used for further experiments. The presence of wild-type vimentin has been shown to enhance cell motility in a PKCe-dependent manner. When these sites are substituted with alanine, vimentin can no longer induce cell motility, while aspartate substitutions allow motility in PKCe null cells. These PKC-mediated phosphorylation sites on vimentin are very important in integrin trafficking through the cell (Ivaska et al., 2005), and the ability of vimentin to assemble into polymers is largely regulated by phosphorylation (Inagaki, Inagaki, Takahashi, & Takai, 1997). Additionally, the expression of vimentin is associated with increased migration of cells involved in EMT (Kang & Massague, 2004). We examined the level of keratin 14 in cells that co-express vimentin. Our western blot analysis shows that the overexpression of vimentin in HN4 cells has an effect on the expression of keratin 14 protein. The amount of keratin 14 appears to be decreased in the cells expressing the wild-type version of vimentin or the PKCe-phosphomimetic version of vimentin when compared to the control HN4V cells. The cells with the unphosphorylatable version of vimentin have an increased level of keratin 14 protein compared to the control HN4V cells. These results suggest that the overexpression of vimentin is having an effect on the expression of keratin 14 in HN4 cells. Additionally, the phosphorylation status of vimentin likely plays a role in this differential keratin 14 expression. However, the results of our qRT-PCR experiments suggest that the expression of the unphosphorylatable version of vimentin in HN4 cells leads to a substantial reduction in the level of keratin 14 mRNA. There is less transcription of keratin 14 in the cells encoding the unphosphorylatable version of vimentin, but the protein may be more stable leading to

enhanced levels of protein seen in the western blot and immunofluorescence experiments. This may be a consequence of the differential vimentin phosphorylation and suggests that the unphosphorylatable version of vimentin may stabilize the protein directly or indirectly. As mentioned above, Ivaska and co-workers found that PKCe-mediated phosphorylation of vimentin controls endocytic vesicle association with intermediate filaments, which is responsible for recycling endocytosed integrins to the plasma membrane, and the substitution of alanine at the PKC-regulated N-terminal phosphorylation sites removes the capability of vimentin to initiate cell motility in PKCe-expressing cells (Ivaska et al., 2005). Once an effect was seen on keratin 14 expression by western blotting and qRT-PCR, we decided to look at the presence of vimentin and keratin 14 by immunofluorescence. Vimentin staining was not present in the control HN4 vector transfected cells, but the staining was clear in the cells encoding the wild-type, PKCe-phosphomimetic, or unphosphorylatable versions of vimentin. Vimentin staining in HN12 shows distinct filaments. However, the staining seen in the mutants differs from this filamentous appearance. The cells encoding the unphosphorylatable version of vimentin has the most distinct staining. Instead of a filament structure, these cells show vimentin in small packets. The cells encoding the PKCe-phosphomimetic version of vimentin has staining that closely resembles HN12. However, the vimentin appears as "squiggles" instead of long filaments. These "squiggles" are thought to be precursors to the longer intermediate filaments that are seen in fibroblasts. The changes in filament structure seen by Ghosh et al. were the result of changes in integrin expression that affected ERK activation (Ghosh et al., 2002). This suggests that mutations at the PKCe-phosphorylation

sites cause defects in intermediate filament assembly. The differences in the appearance of vimentin may be a result of the phosphorylation site substitutions. We also found that all three mutant cell lines clearly expressed keratin 14. The keratin 14 expression in the cells encoding wild-type vimentin or the PKCe-phosphomimetic version of vimentin resembled the staining in the HN4V cells. The cells encoding the unphosphorylatable version of vimentin displayed a different pattern of keratin 14 staining. As seen with vimentin, these cells express keratin 14 in small packets as opposed to filaments. This further suggests that these mutated phosphorylation sites play a role in intermediate filament structure and/or assembly and/or trafficking.

Overexpression of Vimentin is Important in HN4 Biological Properties

In order to determine whether the overexpression of vimentin affects the phenotype of HN4 cells, we assessed the growth of HN4 vimentin transfectants using MTT assays and cell counting. The cells with the wild-type or PKCe-phosphomimetic versions of vimentin showed a significant increase in growth when compared to the HN4V cells. Additionally, the cells with the unphosphorylatable version of vimentin showed a growth level very similar to the HN4V cells. These results suggest that vimentin phosphorylation might contribute positively to cell growth. A wound-closure (scratch) assay was performed on these cells as well, to test if the expression of vimentin altered or affected cell motility. We found that cells expressing the wild-type or PKCe-phosphomimetic versions of vimentin migrated at a faster rate than the HN4V cells and the cells with the unphosphorylatable version of vimentin. Thus, in addition to effects on proliferation, the

ability to phosphorylate vimentin plays a part in cell motility. Other studies have shown that blocking vimentin in breast, head and neck, or colon cancer cells has significantly affected motility and migration. Integrins are important in communication between the cells and the extracellular matrix, and the pattern of integrins is frequently altered during tumor progression (Zhang et al., 2009). For example, squamous carcinoma cells that have increased proliferation frequently express higher levels of $a_6ß_4$. When $a_6ß_4$ integrin binds to an extracellular ligand, it is phosphorylated on tyrosine residues and combines with the adaptor proteins Shc and Grb2. This leads to activation of Ras, which causes activation of both Ras-Erk and Rac-Jnk signaling pathways. These pathways mediate immediate-early gene transcription and cell cycle progression (Mainiero et al., 1997). Additionally, Ras is capable of signaling through PI3K and Rho GTPases, which can work together with transforming growth factor-ß to induce EMT (Guarino, 2007). Based on studies by Ivaska et al. (2005), altered phosphorylation of vimentin may influence integrin signaling and, thus, impact growth and motility.

Effect of Vimentin Expression on E-cadherin in HN4 Cells

E-cadherin is a calcium-binding transmembrane glycoprotein. The extracellular domain interacts with adjacent cell receptors, and the intracellular domain interacts with catenins. E-cadherin is the major molecule in the adherens junction, and it plays an important role in EMT because of its interaction with ß-catenin (Voulgari & Pintzas, 2009). ß-catenin interacts directly with the cytoplasmic N-terminal domain of E-cadherin (Ziober et al., 2001). In tumorigenesis, E-cadherin is frequently inactivated or silenced by

various mechanisms., including repression by transcription factors ZEB1 and ZEB2 (Korpal, Lee, Hu, & Kang, 2008).

We decided to investigate the presence of E-cadherin in the HN4 cells with vimentin overexpression. E-cadherin was present in all four cells lines, but the appearance of E-cadherin was varied. The E-cadherin staining in the cells encoding the wild-type version of vimentin was most similar to the HN4V cells. The cells with the PKCe-phosphomimetic version of vimentin showed E-cadherin in the cytoplasm, but it was also contained in isolated packets. These packets were consistent amongst the entire sample. The E-cadherin staining in the cells containing the unphosphorylatable version of vimentin was very diverse. Some of these cells displayed E-cadherin in packets as seen in the cells with the PKCe-phosphomimetic version of vimentin. Another observation in these cells was slight polarization of the E-cadherin. Again, this polarization was only seen in the altered E-cadherin. Others showed the E-cadherin in large packets. The E-cadherin expression was clearly disrupted.

One study of HNSCC cells showed that activation of Src, a protein tyrosine kinase, was correlated with decreased expression of E-cadherin and the detection of vimentin. The expression of E-cadherin in well-differentiated tumors was found with weak p-Src expression and a lack of vimentin expression. However, high levels of activated Src and the presence of vimentin were found in poorly-differentiated tumors, along with a lack of E-cadherin expression. This study also demonstrated that E-cadherin was expressed in the membrane and cytoplasm in some carcinomas, which indicates qualitative and quantitative changes in tumor cell expression of E-cadherin (Mandal et al., 2008). It is possible that E-

cadherin is present, but the junctional complex is defective, which allows for the cells to be more invasive (Ziober et al., 2001). Other studies have shown that while expression of E-cadherin remained relatively constant in oral squamous cell carcinoma cells, the expression of intermediate filaments and integrins did change (Ghosh et al., 2002).

Inhibition of NF-?B Affects Growth in HN12 Cells

Abnormal expression of NF-?B has been described in many cancers, including head and neck, prostate, lung and pancreatic adenocarcinomas and can enhance survival (Min, Eddy, Sherr, & Sonenshein, 2008). Inhibition of NF-?B resulted in decreased proliferation of HN12 cells. It also caused a decrease in vimentin mRNA expression. Reduced proliferation could be a result of the decrease in vimentin expression. However, it is also possible that the decreased proliferation caused by the NF-?B inhibitor is caused by the lack of transcription of other genes regulated by NF-?B. NF-?B regulates genes encoding proteins involved in cell growth, such as cyclin D1 (Min et al., 2008). Cyclin D1 is an important regulator of cell proliferation, and it is commonly up-regulated in tumorigenesis (Witzel, Koh, & Perkins, 2010).

NF-?B transcription factors play an important role in head and neck cancers, and they are commonly overexpressed in these cancers. 85% of HNSCC patients have shown increased nuclear localization of NF-?B (Stadler et al., 2008). Active NF-?B is found in the nucleus, and it can be inhibited by I?B keeping it contained in the cytoplasm. The transcription of several genes is regulated by NF-?B, including cytokines, growth factors, cell adhesion molecules, and pro-/antiapoptotic proteins (Lee et al., 2007). Studies have

also shown that NF-?B transcription factors are able to repress keratin expression (Blumenberg, 2006). Since these NF-?B transcription factors are frequently present in metastatic cells, we were interested in determining the effect of an NF-?B inhibitor on HN12 cells. Other studies have shown inhibition of NF-?B resulting in inhibited tumor cell survival, proliferation, migration, angiogenesis, and tumorigenesis in squamous cell carcinoma (Loercher et al., 2004).

5-Aza-dC Affects Growth of HN12 Cells

The Wnt signaling pathway is able to promote tumor growth by altering cell proliferation and differentiation. DKK3 is a Wnt antagonist, and when Wnt signaling is inhibited, ß-catenin is phosphorylated and targeted for degradation. The catenins are responsible for transduction of extracellular contacts between cadherins during epithelial reorganization. ß-catenin is able to translocate to the nucleus where it affects gene transcription, and recent studies have shown that it can also act as an oncogene. There are reports of high ß-catenin expression in both colon carcinoma cells and melanoma cells (Ziober et al., 2001). ß-catenin staining in normal fibroblasts and endothelial cells is restricted to the cytoplasm and/or cell membranes. In normal epithelial cells, it is found only in the cell membrane, and it is predominantly located in the nucleus of mesenchymal cells (Voulgari & Pintzas, 2009). ß-catenin accumulation in the cytoplasm and translocation to the nucleus is associated with epithelial cell migration and processes involved in EMT (Gilles et al., 2003). Studies have shown that DKK3 is expressed in normal adult tissues, but the DKK3 gene is repressed in several human cancer cell lines

(Yu et al., 2009). Previous research in our lab showed reduced expression of DKK3 in HN12 cells (Miyazaki et al., 2006). Thus, we wanted to investigate the effect of 5-Aza-dC on HN12 cells to determine if cell growth was altered by the presence of this demethylating agent. The presence of 5-Aza-dC should remove the methylation repression on DKK3 and allow DKK3 to inhibit Wnt signaling in these cells. Our results show a decrease in cell growth as a result of treatment with 5-Aza-dC. The re-expression of DKK3 to inhibit Wnt signaling and prevent ß-catenin translocation to the nucleus in these HN12 cells may have contributed to this decrease in cell growth.

Some cancers exhibit decreased DKK3 expression due to hypermethylation of the promoter (Kobayashi et al., 2002). DKK3 expression is commonly repressed in gastric and colorectal cancers due to promoter methylation, and this is correlated with poor patient prognosis. When heavily methylated and silenced cell lines from colon and gastric cancer were treated with 5-Aza-dC, a demethylating agent that inhibits DNA-methyltransferase activity, and trichostatin A (histone deacetylase inhibitor), the expression of DKK3 was restored. This implies that CpG methylation was responsible for DKK3 repression in these cells. DKK3 expression has caused growth inhibition in lung cancer cells, osteosarcoma cells, and digestive cancer cells, which suggests DKK3 may function as a tumor suppressor (Yu et al., 2009).

After observing a decrease in growth of HN12 cells in the presence of NF-?B inhibitor or 5-Aza-dC, we wanted to determine the combined effect on HN12 cells. Cell growth was decreased in cells grown in the presence of both NF-?B inhibitor and 5-Aza-dC. However, no additive effect was apparent. Instead, the decrease seen with both

treatments resembled the treatment with the NF-?B inhibitor alone. This suggests that they may target the same pathway. This is consistent with previous studies, which show that in Wnt signaling when GSK-3ß is inhibited, the NF-?B inhibitor, I?Ba, is targeted by ubiquitin for destruction (Bachelder, Yoon, Franci, de Herreros, & Mercurio, 2005). This suggests that Wnt signaling could activate NF-?B. However, further study could be done using a smaller concentration of the NF-?B inhibitor. This would eliminate the possibility of maximum inhibition being achieved by NF-?B inhibitor alone.

Additionally, we investigated vimentin expression in HN12 cells treated with the NF-?B inhibitor, 5-Aza-dC, or a combined treatment. Our western blot showed decreased vimentin expression in HN12 cells treated with all three conditions. Treatment with 5-Aza-dC showed the largest decrease in vimentin expression, but the decrease seen with treatment of the NF-?B inhibitor or the NF-?B inhibitor combined with 5-Aza-dC was very similar. We also observed a change in vimentin expression using immunofluorescence. The control HN12 cells showed vimentin filaments throughout the cytoplasm. However, this filament structure was altered in HN12 cells treated with NF-?B inhibitor or 5-Aza-dC. First, vimentin expression was decreased under all three conditions. Secondly, vimentin was not expressed in long filaments. Instead, the staining showed short squiggles, which suggests that vimentin filament assembly was disrupted. These findings are consistent with our hypothesis that Wnt signaling plays a role in vimentin expression during EMT. When the Wnt signaling pathway is inhibited, by removing promoter methylation on DKK3 with 5-Aza-dC treatment, the level of vimentin expression is decreased.

DKK3 Knockdown in Vimentin-negative HN4 Cells

HN4 cells were previously generated in our lab that express DKK3 shRNA. The clones displaying the largest inhibition of DKK3 were chosen for further study. We performed a western blot to confirm the DKK3 knockdown, and we also determined vimentin expression in these cell lines. Our results showed vimentin expression in HN12 and HN4 shDKK3 #1 cells. This supports our hypothesis that Wnt signaling plays a role in vimentin expression. By inhibiting DKK3, Wnt signaling was activated in these HN4 shDKK3 #1 cells and vimentin was expressed. The presence of vimentin was not detected in the HN4 cells. Vimentin expression was not present in the HN4 shDKK3 #4 cells either, which is not surprising since our western blot showed this was not a strong DKK3 knockdown. Since DKK3 is a secreted glycoprotein, conditioned medium was collected from HN4 and HN4 shDKK3 cells and immunoprecipitated with a DKK3 antibody to determine DKK3 secretion from these cells. Studies done in human islet cells have shown that DKK3 expression in pancreatic B cells is characteristic of a secreted protein (Welters & Kulkarni, 2008). Our immunoprecipitation showed secretion of DKK3 in the HN4 and HN4 shDKK3 medium. Although the expression was low, the level seen in the HN4 shDKK3 conditioned medium was reduced compared to the HN4 cells. Further study will need to examine the effect of DKK3 repression on keratin 14 expression.

Future Studies

In this study, we have shown that overexpression of vimentin in vimentin-negative HN4 cells causes changes in cell growth, motility, and keratin 14 expression. These changes may be due to altered vimentin phosphorylation. To determine that PKC phosphorylation of vimentin is responsible for these biological changes, these vimentin overexpressing cells could be treated with a PKC inhibitor, such as bisindolylmaleimide I (BIM-I). Studying proliferation and migration in cells treated with BIM-I would allow us to determine if the effects of vimentin overexpression can be overridden. However, to determine whether vimentin is causing keratin 14 changes at the gene expression level, we could perform a promoter deletion assay. This would allow us to determine the regions of the keratin promoter necessary for transcriptional repression. We could also perform a chromatin immunoprecipitation (ChIP) assay to determine whether specific transcription factors are bound to the keratin promoter. Additionally, we could investigate whether the overexpression of vimentin and inhibition of keratin have a combined effect on EMT. For example, keratin expression could be repressed using shRNA.

Immunofluorescence showed altered E-cadherin expression in the HN4 cells with vimentin overexpression. This suggests that mutations in these vimentin phosphorylation sites can affect junctional proteins. Further investigation of E-cadherin by western blot and qRT-PCR would determine whether expression is increased or decreased in these cells. Additionally, the levels of E-cadherin should be assessed when these cells are treated with BIM-I.

Our study also revealed HN12 cells grown in the presence of a NF-?B inhibitor or 5-Aza-dC showed decreased growth. We are interested in determining whether the result seen with the combined presence of the NF-?B inhibitor and 5-Aza-dC is due to the high concentration of NF-?B inhibitor. To investigate this, we will use a lower concentration of the NF-?B inhibitor, since it showed a similar effect on growth when compared to 5-Aza-dC. If the two treatments are synergistic, there should be a decreased level of growth that is smaller than what is observed with the individual treatments of the NF-?B inhibitor or 5-Aza-dC.

Additionally, we should investigate the effects of NF-?B inhibitor and 5-Aza-dC treatments on vimentin and keratin 14 expression in HN12 cells. This can be explored using a variety of techniques, such as western blotting, qRT-PCR, and immunofluorescence. We would predict that 5-Aza-dC would remove the methylation repression on the Wnt antagonist DKK3 and block Wnt signaling in these HN12 cells. Since this would be expected to cause degradation of ß-catenin, we should compare the level of ß-catenin in HN12 cells and HN12 cells treated with 5-Aza-dC. We could assess the presence of ß-catenin by western blotting and immunofluorescence. Repression of ß-catenin in these HN12 cells should result in a decrease of vimentin expression and an increase of keratin 14 expression.

Furthermore, inhibiting DKK3 expression in HN4 cells should activate Wnt signaling in these vimentin-negative cells. We would like to explore the effect of repressed DKK3 expression on vimentin, keratin 14, and ß-catenin expression in HN4 cells. These experiments would allow us to further determine the role of Wnt signaling in EMT.

Literature Cited

## Literature Cited

Allen, C. T., Ricker, J. L., Chen, Z., & Van Waes, C. (2007). Role of activated nuclear factor-kappaB in the pathogenesis and therapy of squamous cell carcinoma of the head and neck. *Head & Neck, 29*(10), 959-971.

Bachelder, R. E., Yoon, S. O., Franci, C., de Herreros, A. G., & Mercurio, A. M. (2005). Glycogen synthase kinase-3 is an endogenous inhibitor of snail transcription: Implications for the epithelial-mesenchymal transition. *The Journal of Cell Biology, 168*(1), 29-33.

Blumenberg, M. (2006). Transcriptional regulation of keratin gene expression. *Intermediate filaments* (pp. 93-109). New York, N.Y.: Springer Science.

Chu, P. G., & Weiss, L. M. (2002). Keratin expression in human tissues and neoplasms. *Histopathology, 40*(5), 403-439.

Dissanayake, S. K., Wade, M., Johnson, C. E., O'Connell, M. P., Leotlela, P. D., French, A. D., et al. (2007). The Wnt5A/protein kinase C pathway mediates motility in melanoma cells via the inhibition of metastasis suppressors and initiation of an epithelial to mesenchymal transition. *The Journal of Biological Chemistry, 282*(23), 17259-17271.

Du, Q., Zhang, X., Cardinal, J., Cao, Z., Guo, Z., Shao, L., et al. (2009). Wnt/beta-catenin signaling regulates cytokine-induced human inducible nitric oxide synthase expression by inhibiting nuclear factor-kappaB activation in cancer cells. *Cancer Research, 69*(9), 3764-3771.

Eriksson, J. E., Brautigan, D. L., Vallee, R., Olmsted, J., Fujiki, H., & Goldman, R. D. (1992). Cytoskeletal integrity in interphase cells requires protein phosphatase activity. *Proceedings of the National Academy of Sciences of the United States of America, 89*(22), 11093-11097.

Eriksson, J. E., He, T., Trejo-Skalli, A. V., Harmala-Brasken, A. S., Hellman, J., Chou, Y. H., et al. (2004). Specific in vivo phosphorylation sites determine the assembly dynamics of vimentin intermediate filaments. *Journal of Cell Science, 117*(Pt 6), 919-932.

Ferris, R. L., & Grandis, J. R. (2007). NF-kappaB gene signatures and p53 mutations in head and neck squamous cell carcinoma. *Clinical Cancer Research : An Official Journal of the American Association for Cancer Research, 13*(19), 5663-5664.

Ghosh, S., Munshi, H. G., Sen, R., Linz-McGillem, L. A., Goldman, R. D., Lorch, J., et al. (2002). Loss of adhesion-regulated proteinase production is correlated with invasive activity in oral squamous cell carcinoma. *Cancer, 95*(12), 2524-2533.

Gilles, C., Polette, M., Mestdagt, M., Nawrocki-Raby, B., Ruggeri, P., Birembaut, P., et al. (2003). Transactivation of vimentin by beta-catenin in human breast cancer cells. *Cancer Research, 63*(10), 2658-2664.

Gilles, C., Polette, M., Piette, J., Delvigne, A. C., Thompson, E. W., Foidart, J. M., et al. (1996). Vimentin expression in cervical carcinomas: Association with invasive and migratory potential. *The Journal of Pathology, 180*(2), 175-180.

Goto, H., Kosako, H., Tanabe, K., Yanagida, M., Sakurai, M., Amano, M., et al. (1998). Phosphorylation of vimentin by rho-associated kinase at a unique amino-terminal site that is specifically phosphorylated during cytokinesis. *The Journal of Biological Chemistry, 273*(19), 11728-11736.

Goto, H., Yasui, Y., Kawajiri, A., Nigg, E. A., Terada, Y., Tatsuka, M., et al. (2003). Aurora-B regulates the cleavage furrow-specific vimentin phosphorylation in the cytokinetic process. *The Journal of Biological Chemistry, 278*(10), 8526-8530.

Gu, L. H., & Coulombe, P. A. (2007). Keratin function in skin epithelia: A broadening palette with surprising shades. *Current Opinion in Cell Biology, 19*(1), 13-23.

Guarino, M. (2007). Epithelial-mesenchymal transition and tumour invasion. *The International Journal of Biochemistry & Cell Biology, 39*(12), 2153-2160.

Gyoeva, F. K., & Gelfand, V. I. (1991). Coalignment of vimentin intermediate filaments with microtubules depends on kinesin. *Nature, 353*(6343), 445-448.

Hanahan, D., & Weinberg, R. A. (2000). The hallmarks of cancer. *Cell, 100*(1), 57-70.

Hollier, B. G., Evans, K., & Mani, S. A. (2009). The epithelial-to-mesenchymal transition and cancer stem cells: A coalition against cancer therapies. *Journal of Mammary Gland Biology and Neoplasia, 14*(1), 29-43.

Howe, L. R., Watanabe, O., Leonard, J., & Brown, A. M. (2003). Twist is up-regulated in response to Wnt1 and inhibits mouse mammary cell differentiation. *Cancer Research, 63*(8), 1906-1913.

Howell, G. M., & Grandis, J. R. (2005). Molecular mediators of metastasis in head and neck squamous cell carcinoma. *Head & Neck, 27*(8), 710-717.

Inagaki, M., Inagaki, N., Takahashi, T., & Takai, Y. (1997). Phosphorylation-dependent control of structures of intermediate filaments: A novel approach using site- and phosphorylation state-specific antibodies. *Journal of Biochemistry, 121*(3), 407-414.

Ivaska, J., Vuoriluoto, K., Huovinen, T., Izawa, I., Inagaki, M., & Parker, P. J. (2005). PKCepsilon-mediated phosphorylation of vimentin controls integrin recycling and motility. *The EMBO Journal, 24*(22), 3834-3845.

Ivaska, J., Whelan, R. D., Watson, R., & Parker, P. J. (2002). PKC epsilon controls the traffic of beta1 integrins in motile cells. *The EMBO Journal, 21*(14), 3608-3619.

Janssens, N., Janicot, M., & Perera, T. (2006). The wnt-dependent signaling pathways as target in oncology drug discovery. *Investigational New Drugs, 24*(4), 263-280.

Kang, Y., & Massague, J. (2004). Epithelial-mesenchymal transitions: Twist in development and metastasis. *Cell, 118*(3), 277-279.

Karin, M., Cao, Y., Greten, F. R., & Li, Z. W. (2002). NF-kappaB in cancer: From innocent bystander to major culprit. *Nature Reviews.Cancer, 2*(4), 301-310.

Kim, J. K., & Diehl, J. A. (2009). Nuclear cyclin D1: An oncogenic driver in human cancer. *Journal of Cellular Physiology, 220*(2), 292-296.

Kobayashi, K., Ouchida, M., Tsuji, T., Hanafusa, H., Miyazaki, M., Namba, M., et al. (2002). Reduced expression of the REIC/Dkk-3 gene by promoter-hypermethylation in human tumor cells. *Gene, 282*(1-2), 151-158.

Korpal, M., Lee, E. S., Hu, G., & Kang, Y. (2008). The miR-200 family inhibits epithelial-mesenchymal transition and cancer cell migration by direct targeting of E-cadherin transcriptional repressors ZEB1 and ZEB2. *The Journal of Biological Chemistry, 283*(22), 14910-14914.

Kramer, R. H., Shen, X., & Zhou, H. (2005). Tumor cell invasion and survival in head and neck cancer. *Cancer Metastasis Reviews, 24*(1), 35-45.

Kühl, M. (2003). *Wnt signaling in development*. Georgetown, Tex.; New York: Landes Bioscience; Kluwer Academic/Plenum.

Lee, C. H., Jeon, Y. T., Kim, S. H., & Song, Y. S. (2007). NF-kappaB as a potential molecular target for cancer therapy. *BioFactors (Oxford, England), 29*(1), 19-35.

Lehninger, A. L., Nelson, D. L., & Cox, M. M. (2005). *Lehninger principles of biochemistry* (4th ed.). New York: W.H. Freeman.

Lester, R. D., Jo, M., Montel, V., Takimoto, S., & Gonias, S. L. (2007). uPAR induces epithelial-mesenchymal transition in hypoxic breast cancer cells. *The Journal of Cell Biology, 178*(3), 425-436.

Levayer, R., & Lecuit, T. (2008). Breaking down EMT. *Nature Cell Biology, 10*(7), 757-759.

Liao, J., & Omary, M. B. (1996). 14-3-3 proteins associate with phosphorylated simple epithelial keratins during cell cycle progression and act as a solubility cofactor. *The Journal of Cell Biology, 133*(2), 345-357.

Lodish, H. F. (2004). *Molecular cell biology* (5th ed.). New York: W.H. Freeman and Co.

Loercher, A., Lee, T. L., Ricker, J. L., Howard, A., Geoghegen, J., Chen, Z., et al. (2004). Nuclear factor-kappaB is an important modulator of the altered gene expression profile and malignant phenotype in squamous cell carcinoma. *Cancer Research, 64*(18), 6511-6523.

Lyons, A. J., & Jones, J. (2007). Cell adhesion molecules, the extracellular matrix and oral squamous carcinoma. *International Journal of Oral and Maxillofacial Surgery, 36*(8), 671-679.

Mainiero, F., Murgia, C., Wary, K. K., Curatola, A. M., Pepe, A., Blumemberg, M., et al. (1997). The coupling of alpha6beta4 integrin to ras-MAP kinase pathways mediated by shc controls keratinocyte proliferation. *The EMBO Journal, 16*(9), 2365-2375.

Mandal, M., Myers, J. N., Lippman, S. M., Johnson, F. M., Williams, M. D., Rayala, S., et al. (2008). Epithelial to mesenchymal transition in head and neck squamous carcinoma: Association of src activation with E-cadherin down-regulation, vimentin expression, and aggressive tumor features. *Cancer, 112*(9), 2088-2100.

Min, C., Eddy, S. F., Sherr, D. H., & Sonenshein, G. E. (2008). NF-kappaB and epithelial to mesenchymal transition of cancer. *Journal of Cellular Biochemistry, 104*(3), 733-744.

Minin, A. A., & Moldaver, M. V. (2008). Intermediate vimentin filaments and their role in intracellular organelle distribution. *Biochemistry.Biokhimiia, 73*(13), 1453-1466.

Miyazaki, H., Patel, V., Wang, H., Edmunds, R. K., Gutkind, J. S., & Yeudall, W. A. (2006). Down-regulation of CXCL5 inhibits squamous carcinogenesis. *Cancer Research, 66*(8), 4279-4284.

Muir, R., & Anderson, J. R. (1985). *Muir's textbook of pathology* [Textbook of pathology] (12th ed.). London ; Baltimore, Md., U.S.A.: Arnold.

*Oral cancer*. (2009). Retrieved December, 2009, from http://www.cancer.org/downloads/PRO/OralCancer.pdf

Paccione, R. J., Miyazaki, H., Patel, V., Waseem, A., Gutkind, J. S., Zehner, Z. E., et al. (2008). Keratin down-regulation in vimentin-positive cancer cells is reversible by

vimentin RNA interference, which inhibits growth and motility. *Molecular Cancer Therapeutics, 7*(9), 2894-2903.

Palmieri, G., Capone, M., Ascierto, M. L., Gentilcore, G., Stroncek, D. F., Casula, M., et al. (2009). Main roads to melanoma. *Journal of Translational Medicine, 7*, 86.

Paramio, J. M. (2006). *Intermediate filaments*. Georgetown, Tex.; New York, N.Y.: Landes Bioscience/Eurekah.com; Springer Science+Business Media.

Parry, D. A. D., & Steinert, P. M. (1995). *Intermediate filament structure*. Austin, Tex.: R.G. Landes.

Pendas-Franco, N., Aguilera, O., Pereira, F., Gonzalez-Sancho, J. M., & Munoz, A. (2008). Vitamin D and Wnt/beta-catenin pathway in colon cancer: Role and regulation of DICKKOPF genes. *Anticancer Research, 28*(5A), 2613-2623.

Rapidis, A. D., & Wolf, G. T. (2009). Immunotherapy of head and neck cancer: Current and future considerations. *Journal of Oncology, 2009*, 346345.

Saeb-Parsy, K., Veerakumarasivam, A., Wallard, M. J., Thorne, N., Kawano, Y., Murphy, G., et al. (2008). MT1-MMP regulates urothelial cell invasion via transcriptional regulation of dickkopf-3. *British Journal of Cancer, 99*(4), 663-669.

Singh, S., Sadacharan, S., Su, S., Belldegrun, A., Persad, S., & Singh, G. (2003). Overexpression of vimentin: Role in the invasive phenotype in an androgen-independent model of prostate cancer. *Cancer Research, 63*(9), 2306-2311.

Stadler, M. E., Patel, M. R., Couch, M. E., & Hayes, D. N. (2008). Molecular biology of head and neck cancer: Risks and pathways. *Hematology/oncology Clinics of North America, 22*(6), 1099-124, vii.

Voulgari, A., & Pintzas, A. (2009). Epithelial-mesenchymal transition in cancer metastasis: Mechanisms, markers and strategies to overcome drug resistance in the clinic. *Biochimica Et Biophysica Acta, 1796*(2), 75-90.

Welters, H. J., & Kulkarni, R. N. (2008). Wnt signaling: Relevance to beta-cell biology and diabetes. *Trends in Endocrinology and Metabolism: TEM, 19*(10), 349-355.

Witzel, I. I., Koh, L. F., & Perkins, N. D. (2010). Regulation of cyclin D1 gene expression. *Biochemical Society Transactions, 38*(Pt 1), 217-222.

Woods, A. J., White, D. P., Caswell, P. T., & Norman, J. C. (2004). PKD1/PKCmu promotes alphavbeta3 integrin recycling and delivery to nascent focal adhesions. *The EMBO Journal, 23*(13), 2531-2543.

Yeudall, W. A., Miyazaki, H., Ensley, J. F., Cardinali, M., Gutkind, J. S., & Patel, V. (2005). Uncoupling of epidermal growth factor-dependent proliferation and invasion in a model of squamous carcinoma progression. *Oral Oncology, 41*(7), 698-708.

Yu, J., Tao, Q., Cheng, Y. Y., Lee, K. Y., Ng, S. S., Cheung, K. F., et al. (2009). Promoter methylation of the Wnt/beta-catenin signaling antagonist dkk-3 is associated with poor survival in gastric cancer. *Cancer, 115*(1), 49-60.

Zhang, X., Fournier, M. V., Ware, J. L., Bissell, M. J., Yacoub, A., & Zehner, Z. E. (2009). Inhibition of vimentin or beta1 integrin reverts morphology of prostate tumor cells grown in laminin-rich extracellular matrix gels and reduces tumor growth in vivo. *Molecular Cancer Therapeutics, 8*(3), 499-508.

Zhou, Z., Kahns, S., & Nielsen, A. L. (2009). Identification of a novel vimentin promoter and mRNA isoform. *Molecular Biology Reports,*

Ziober, B. L., Silverman, S. S.,Jr, & Kramer, R. H. (2001). Adhesive mechanisms regulating invasion and metastasis in oral cancer. *Critical Reviews in Oral Biology and Medicine : An Official Publication of the American Association of Oral Biologists, 12*(6), 499-510.

# VITA

Mary Catherine McGinn was born on September 5, 1985, in Martinsville, Virginia to the parents of Dr. and Mrs. James S. McGinn. She graduated from Martinsville High School in 2003 as valedictorian. She received her Bachelor of Science degree in Kinesiology and minored in Music at The College of William and Mary, Williamsburg, Virginia in 2007. In pursuit of her Master of Science degree at Virginia Commonwealth University, she received the Department of Physiology Poland Award. In August 2010, Mary Catherine enrolled at Virginia Commonwealth University School of Dentistry Class of 2014.

.